

# ICASE

ND 210491  
NACI-258

A SPLINE-BASED PARAMETER AND STATE ESTIMATION TECHNIQUE  
FOR STATIC MODELS OF ELASTIC SURFACES

IN-64  
64388

H. T. Banks  
P. L. Daniel  
E. S. Armstrong

LIBRARY COPY

Report No. 83-25

June 28, 1983

NOV 20 1986

LANGLEY RESEARCH CENTER  
LIBRARY, NASA  
HAMPTON, VIRGINIA

(NASA-CR-180449) A SPLINE-BASED PARAMETER  
AND STATE ESTIMATION TECHNIQUE FOR STATIC  
MODELS OF ELASTIC SURFACES (NASA) 62 p  
Avail: NTIS HC A04/MF A01

N87-30107

CSCL 12A

Unclass

G3/64 0064388

INSTITUTE FOR COMPUTER APPLICATIONS IN SCIENCE AND ENGINEERING  
NASA Langley Research Center, Hampton, Virginia 23665

Operated by the

UNIVERSITIES SPACE



RESEARCH ASSOCIATION

A Spline-Based Parameter and State Estimation Technique  
For Static Models of Elastic Surfaces

May, 1983

H. T. Banks  
Lefschetz Center for Dynamical Systems  
Division of Applied Mathematics  
Brown University  
Providence, RI 02912

B1720314

P. L. Daniel  
Department of Mathematics  
Southern Methodist University  
Dallas, TX 75275

55949356

E. S. Armstrong  
Spacecraft Control Branch  
Flight Dynamics and Control Division  
NASA Langley Research Center  
Hampton, VA 23665

Abstract

We discuss parameter and state estimation techniques for an elliptic system arising in a developmental model for the antenna surface in the Maypole Hoop/Column antenna. A computational algorithm based on spline approximations for the state and elastic parameters is given and numerical results obtained using this algorithm are summarized.

Research reported here was supported in part by NASA Grant NAG-1-258 for the first and second authors, in part by NSF Grant MCS-8205355 and in part by AFOSR Grant 81-0198 for the first author, and NSF Grant MCS-8200883 for the second author. Parts of the efforts reported were carried out while the first two authors were in residence at the Institute for Computer Applications in Science and Engineering, NASA Langley Research Center, Hampton, VA, which is operated under NASA Contracts No. NAS1-15810 and No. NAS1-16394.

## I. Introduction

Proposed large space structures have many characteristics that make them difficult to analyze and control [1]. They are typically highly flexible--with components mathematically modeled by partial differential equations or very large systems of ordinary differential equations. They have many resonant frequencies--possibly low and closely spaced. Natural damping may be low and/or improperly modeled [2]. Coupled with stringent operational requirements of orientation, shape control, and vibration suppression, and the inability to perform adequate ground testing, these characteristics present an unconventional control design problem to the systems theorist.

Frequently, linear multivariable control theory is applied to reduced order models obtained from finite element software with the goal of controlling the structure so as to meet the operational requirements without overly exciting higher order modes. Difficulties can arise essentially from the process of analyzing and designing controllers for flexible, inherently distributed systems employing lumped parameter models and finite dimensional control methodology. The effects of spillover, modeling error, and insufficient structural damping are well known [1, 3] and may force the designer into low authority control laws with compromised operational performance.

An alternative approach would be to acknowledge the distributed nature of the problem and design the control system using distributed parameter techniques. Many aspects of distributed parameter control theory analogous to multivariable theory exist or are currently being developed [1, 4-7, 7a, 7b, 7c]. Unfortunately, control laws derived from distributed parameter theory usually are infinite-dimensional and often require significant simplification to be realized with current sensor and actuator technology. Although distributed

parameter control methodology may ultimately be applied to large space structures, it is doubtful that first generation large space structures will have sufficient hardware and computer capability to apply the resulting solutions.

However, even at the present time, much can be gained from the distributed parameter approach in the area of parameter estimation. Whether the lumped or distributed parameter control design approach is taken, there remains the underlying need for design models which adequately reflect the structural characteristics and which can be quickly and easily modified to carry out parametric studies [3] and to perform sensitivity and robustness analyses essential to control design [8]. There are also open questions in the understanding and modeling of damping [2, 3] which may be better treated within a distributed parameter formulation. Finally, a distributed model appears to have the potential of facilitating the parameter estimation problem for large scale systems since quantities to be estimated will usually appear explicitly within coefficient functions of the partial differential equations.

This report summarizes some of the results from an ongoing Langley Research Center program directed towards developing parameter estimation techniques for flexible systems modeled by partial differential equations with an emphasis on large space structures. The intent of the program is to produce general purpose techniques with a sound theoretical basis which are computationally efficient while contributing to Langley's technology development program in large space antennas [9]. Of the many techniques available for parameter estimation in distributed systems (for example, see [10]) the spline based estimation techniques of [11-15, 15a] appear well suited for large space structures applications and are currently being developed to treat this class of problems. Simultaneously, an estimation problem associated with the Maypole (Hoop/Column) antenna [16]

is being formulated and will be solved as part of the developmental process. The next section of this paper describes the Hoop/Column antenna and presents the identification problem being considered. The parameter estimation approach is then outlined and discussed in the context of the Hoop/Column application. Subsequent sections include mathematical details of the antenna application and numerical results.

## II. The Maypole (Hoop/Column) Antenna

One of the planned activities of the NASA's Space Transportation System is the placement in earth orbit of a variety of large space antennas. Potential large space missions for the next two decades will require antennas and structures ranging from 30m to 20km in size. Applications include communications (mobile, trunking, etc.), remote sensing (soil moisture, salinity, etc.), deep space network (orbital relays), astronomy (x-ray observatory, optical array, radio telescope, very long baseline interferometry, etc.), energy, and space platforms.

For the purpose of technology development, the NASA Large Scale Systems Technology (LSST) program office has pinpointed focus missions and identified future requirements for large space antennas for communications, earth sensing, and radio astronomy [9]. In this study, particular emphasis is placed on mesh deployable antennas in the 50-120 meter diameter category. Communication satellites of this size will require a pointing accuracy of  $0.035^{\circ}$  and surface accuracy of 4-8mm. One such antenna is the Maypole (Hoop/Column) antenna shown for the 100m point-design in Figures 1, 2, and 6. This antenna concept has been selected by the LSST office for development by the Harris Corporation, Melbourne, Florida, under contract to the Langley Research Center [16].

The Hoop/Column antenna consists of a knitted gold-plated molybdenum wire reflective mesh stretched over a collapsible hoop that supplies the rigidity necessary to maintain a circular outer shape. The mesh grid can be varied to meet a given radio frequency reflectivity requirement. The annular membrane-like reflector surface surrounds a telescoping mast which provides anchoring locations for the mesh center section (Figure 2). The mast also provides anchoring for cables that connect the top end of the mast to the outer hoop and the bottom end of the mast to 48 equally spaced radial graphite cord truss systems woven through the mesh surface [16]. Tensions on the upper (quartz) cables and outer lower (graphite epoxy) cables are counter balanced to provide stiffness to the hoop structure. The inner lower cables produce, through the truss systems, distributed surface loading to control the shape of four circular reflective dishes (Figures 2 and 6) on the mesh surface. Flat, conical, parabolic, or spherical dish surfaces can be produced using this cable drawing technique.

After deployment or after a long period of operation, the reflector surface may require adjustment. Optical sensors are to be located on the upper mast which measure angles of retroreflective targets placed on the truss radial cord edges on the antenna surface. This information can then be processed using a ground-based computer to determine a data set of values of mesh surface location at selected target points. If necessary, a new set of shaping (control) cord tensions can be fed back to the antenna for adjustment.

It is desirable to have an identification procedure which allows one to estimate the antenna mesh shape at arbitrary surface points and the distributed loading from data set observations. It can also be anticipated that environmental stresses and the effects of aging will alter the mesh material properties. The identification procedure must also allow one to address this issue.

It is the intention of the authors to develop identification procedures for use in distributed parameter models of the mesh surface. Considering the antenna to be fully deployed and in static equilibrium, we are currently deriving a mathematical model which describes the antenna surface deviation from a curved equilibrium configuration (for preliminary findings, see [16a]). Using a cylindrical coordinate system with the z axis along the mast, it is expected that the resulting model will entail a system of coupled second order linear partial differential equations in two spatial variables. The coefficients of these equations are functions of the material properties of the stretched mesh. The derivation and computer software for this model are still under development. In the meantime, a simpler developmental (prototype) problem has been solved which is descriptive of the original problem and for which the software produced will hopefully be readily extended for use in the more general case.

For the developmental problem, the loading is assumed to be normal to the plane containing the hoop rim and the mesh surface is assumed to be described by the static two-dimensional stretched membrane equation [17] with variable stiffness (elastic) coefficients and appropriate boundary conditions for the Hoop/Column geometry. (We note that there is ample precedent in the literature [17a, 17b] for use of a scalar Poisson's equation for the two-dimensional stretched membrane as a prototype or developmental model in the study of large space antennas.) Mathematically, in polar coordinates, we have

$$-\frac{1}{r} \frac{\partial}{\partial r} [rE(r, \theta) \frac{\partial u}{\partial r}] - \frac{1}{r^2} \frac{\partial}{\partial \theta} [E(r, \theta) \frac{\partial u}{\partial \theta}] = f(r, \theta) \quad (1)$$

where  $u(r, \theta)$  is the vertical displacement of the mesh from the hoop plane,

$f(r, \theta)$  is the distributed loading force per unit area, and  $E(r, \theta) > 0$  is the distributed stiffness (elastic) coefficient of the mesh surface (force/unit length). Equation (1) is to be solved over the annular region  $\Omega = [\epsilon, R] \times [0, 2\pi]$ . Appropriate boundary conditions are

$$u(\epsilon, \theta) = u_0$$

$$u(R, \theta) = 0 \quad (2)$$

$$u(r, 0) = u(r, 2\pi),$$

where  $R$  is the radius from the mast center to the circular outer hoop,  $\epsilon$  is the radius from the mast to the beginning of the mesh surface (see Figure 6), and  $u_0$  is the coordinate at  $r = \epsilon$  of the mesh surface below the outer hoop plane. For the 100-meter point design antenna, one finds

$$R = 50 \text{ m}$$

$$\epsilon = 8.235 \text{ m} \quad (3)$$

$$u_0 = -7.5 \text{ m}.$$

We further assume that the distributed loading along with a data set of vertical displacements,  $u_m(r_i, \theta_j)$ , at selected points  $(r_i, \theta_j)$  on the mesh surface is known. Given this information, the developmental problem is to estimate the material properties of the mesh as represented by  $E(r, \theta)$  and produce estimates of the surface represented by  $u(r, \theta)$  at arbitrary  $(r, \theta)$  points within  $\Omega$ . The procedure applied to solve this problem is discussed in the next section.

### III. The Parameter Estimation Approximation Scheme

The first two authors and their colleagues have derived techniques for approximating the solutions to systems identification and control problems involving delay equation models and partial differential equation models in one spatial variable and have used them in a variety of applications [18, 18a]. The Hoop/Column application requires an extension of the theory and numerical algorithms to elliptic distributed systems in several spatial variables. The approach, when specialized to the parameter estimation problem, may be summarized as follows. (1) Select a distributed parameter formulation containing unknown parameters for a specific system. (2) Mathematically "project" the formulation down onto a finite dimensional subspace through some approximation procedure such as finite differences, finite elements, etc. (3) Solve the parameter estimation problem within the finite dimensional subspace obtaining a parameter estimate dependent upon the order of the approximation embodied in the subspace. (4) Successively increase the order of the approximation and, in each case, solve the parameter estimation problem so as to construct a sequence of parameter estimates ordered with increasing refinement of the approximation scheme. (5) Seek a mathematical theory which provides conditions under which the sequence of approximate solutions approaches the distributed solution as the subspace dimension increases with a convergent underlying sequence of parameter estimates.

In applying this approach to the developmental problem described in this report, the stiffness function is parametrized in terms of cubic splines which converts the estimation of  $E(r,\theta)$  into a finite dimensional parameter estimation problem. After writing the energy functional generic to the membrane equation, we use the Galerkin procedure to project the distributed

formulation onto a finite dimensional state subspace spanned by tensor products of linear spline functions defined over  $\Omega$ . The approximate displacement thus obtained is expressible in terms of the spline basis functions. The Galerkin procedure in this case yields algebraic equations which define the displacement approximation coordinates in terms of the unknown parameters. In order to solve the approximating parameter estimation problem, the parameters defining  $E(r, \theta)$  are chosen so that a least squares measure of the fit error between the observed and predicted (by the approximate state) data set is minimized. Finally, following steps (4) and (5) an algorithm is constructed to determine the order of the linear spline approximation above which little or no further improvement is obtained in the unknown parameters as one increases the dimension of the subspaces.

Following this procedure, a one-dimensional version of the developmental problem has been solved [19] in which the schemes proposed were successfully tested. Further details of the two-dimensional case follow.

#### IV. Finite Dimensional Approximations

We choose a Galerkin procedure [20, 20a] with linear spline basis functions to perform the finite dimensional approximation for the developmental problem in which  $E(r, \theta)$  and  $u(r, \theta)$  of equation (1) are to be estimated. The boundary conditions (2) are first converted to homogeneous form by introducing the new dependent variable

$$y(r, \theta) = u(r, \theta) - \left( \frac{r-R}{\epsilon-R} \right) u_0 \quad (4)$$

whereby equation (1) becomes

$$-\frac{1}{r} \frac{\partial}{\partial r} [rE(r, \theta) \frac{\partial y}{\partial r}] - \frac{1}{r^2} \frac{\partial}{\partial \theta} [E(r, \theta) \frac{\partial y}{\partial \theta}] = f(r, \theta) + \frac{1}{r} \frac{\partial}{\partial r} \left[ \frac{rE(r, \theta)u_0}{\epsilon - R} \right] \quad (5)$$

with boundary conditions

$$y(\epsilon, \theta) = 0$$

$$y(R, \theta) = 0 \quad (6)$$

$$y(r, 0) = y(r, 2\pi).$$

Following the standard formulation (see [20, 20a]) for the weak or variational form of (5), the energy functional  $\mathcal{E}$  associated with (5) is

$$\mathcal{E}(z) = \int_0^{2\pi} \int_{\epsilon}^R \left\{ \frac{1}{2} E(r, \theta) \nabla z \cdot \nabla z - \tilde{f}(r, \theta) z \right\} r dr d\theta, \quad (7)$$

where  $\nabla$  is the gradient in polar coordinates which, in the form used here, is equivalent to

$$\left( \frac{\partial}{\partial r}, \frac{1}{r} \frac{\partial}{\partial \theta} \right)^T. \quad (8)$$

The function  $\tilde{f}$  is given by

$$\tilde{f}(r, \theta) = f(r, \theta) + \frac{1}{r} \frac{\partial}{\partial r} \left( \frac{rE(r, \theta)u_0}{\epsilon - R} \right) \quad (9)$$

and the vertical displacement  $z(r, \theta)$  of the mesh surface away from the hoop equilibrium plane is a function satisfying the boundary conditions (6) and possessing first derivatives on  $\Omega$  in the mean square sense (we denote this by  $z \in H_0^1, \text{per}(\Omega) \equiv Z$ ). The first variation  $\delta\mathcal{E}$  of  $\mathcal{E}$  about the function  $y(r, \theta)$  is given by

$$\begin{aligned}
 \delta E(y; v) &= \int_0^{2\pi} \int_{\epsilon}^R \left\{ E(r, \theta) v y + v v - f(r, \theta) v \right\} r dr d\theta \\
 &= \int_0^{2\pi} \int_{\epsilon}^R \left\{ E(r, \theta) v y + v v - [f(r, \theta) v + E(r, \theta) \hat{k} \cdot \nabla v] \right\} r dr d\theta \quad (10)
 \end{aligned}$$

where

$$\hat{k} = \begin{pmatrix} \hat{k} \\ 0 \end{pmatrix} = \begin{pmatrix} \frac{u_0}{R-\epsilon} \\ 0 \end{pmatrix}$$

and  $v$  is an arbitrary function in  $Z = H_{0, \text{per}}^1(\Omega)$ .

Under sufficient smoothness assumptions one can integrate by parts in the first term in (10). Then, if one invokes the conditions that  $y$  provides a stationary value for  $E$ , the fact that  $\delta E(y; v)$  vanishes for all  $v$  in  $Z$  yields equation (5). However, we shall not follow this course, but rather we shall apply the Galerkin procedure directly to the weak form of (5) given by  $\delta E(y; v) = 0$ .

Given a finite dimensional subspace  $\hat{Z}$  of  $Z$ , the Galerkin procedure defines the approximation  $\hat{y}$  as the solution in  $\hat{Z}$  of

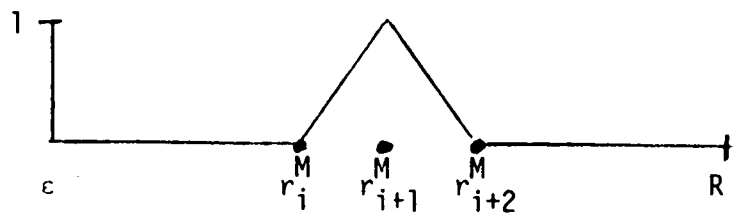
$$\int_0^{2\pi} \int_{\epsilon}^R \left\{ E(r, \theta) \hat{v} y + v v \right\} r dr d\theta = \int_0^{2\pi} \int_{\epsilon}^R \left\{ f(r, \theta) \hat{v} + E(r, \theta) \hat{k} \cdot \nabla \hat{v} \right\} r dr d\theta \quad (12)$$

for all  $\hat{v} \in \hat{Z}$ .

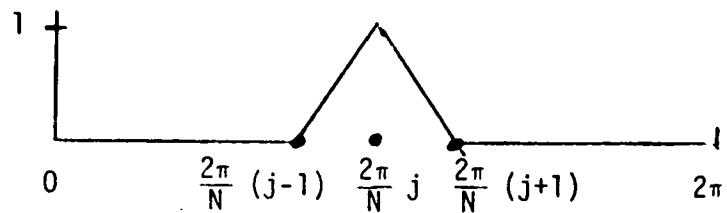
For computational efficiency, the basis functions used for the representations of  $\hat{y}$  in (12) are taken as tensor products of linear B-splines [20, p. 27; 20a, p. 100]. Thus  $\hat{v}$  and  $\hat{y}$  are in the space spanned by  $v_{ij}^{M, N}$ , where

$$v_{ij}^{M,N}(r, \theta) = \alpha_i^M(r) \beta_j^N(\theta), \quad (i = 1, \dots, M-1; \quad j = 1, \dots, N), \quad (13)$$

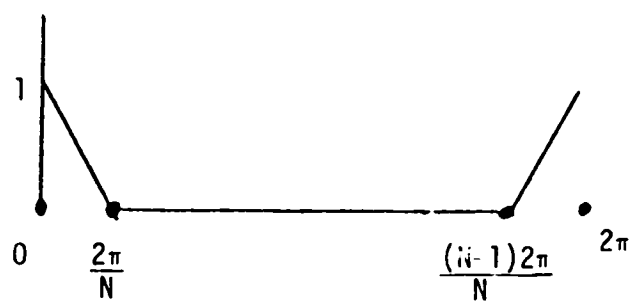
where  $\alpha_i^M$  and  $\beta_j^N$  have the following form: On the interval  $[\epsilon, R]$  (subdivided by defining partition points  $r_j^M = \epsilon + (R-\epsilon)(j-1)/M$ ,  $j = 1, \dots, M+1$ ),  $\alpha_i^M$  is the  $i^{\text{th}}$  linear B-spline basis element,  $i = 1, 2, \dots, M-1$ , given in the following graphical representation



Subdividing  $[0, 2\pi]$  into intervals of uniform length  $2\pi/N$ , we define  $\beta_j^N$  for  $j = 1, \dots, N-1$  by



and define  $\beta_N^N(\theta)$  as follows.



For  $y(r, \theta)$  within the subspace spanned by  $v_{ij}^{M, N}$  we can write

$$y^{M, N}(r, \theta) = \sum_{i=1}^{M-1} \sum_{j=1}^N \alpha_i^M(r) w_{ij}^{M, N} \beta_j^N(\theta) \quad (14)$$

Note that the coordinate  $w_{ij}^{M, N}$  is just the value of  $y^{M, N}(r, \theta)$  at

$$r = \epsilon + \frac{i(R-\epsilon)}{M}$$

$$\theta = \frac{j2\pi}{N}.$$

Replacing  $y(r, \theta)$  in (12) by  $y^{M, N}(r, \theta)$  from (14), (and letting  $v(r, \theta) = v_{ij}^{M, N}(r, \theta)$  for  $i = 1, \dots, M-1; j = 1, \dots, N$ ) we generate the following set of algebraic equations for  $w_{ij}^{M, N}$ .

$$\sum_{i=1}^{M-1} \sum_{j=1}^N w_{ij}^{M, N} K_{k\ell, ij}^{MN} = F_{k\ell}^{MN} + G_{k\ell}^{MN} \quad (k = 1, \dots, M-1; \ell = 1, \dots, N), \quad (15)$$

where

$$\begin{aligned} K_{k\ell, ij}^{MN} &= \int_0^{2\pi} \int_{\epsilon}^R E(r, \theta) v[\alpha_i^M(r) \beta_j^N(\theta)] \cdot v[\alpha_k^M(r) \beta_\ell^N(\theta)] r dr d\theta \\ &= \int_0^{2\pi} \int_{\epsilon}^R E(r, \theta) \beta_j^N(\theta) \beta_\ell^N(\theta) \left[ \frac{d}{dr} \alpha_i^M(r) \right] \left[ \frac{d}{dr} \alpha_k^M(r) \right] r dr d\theta \\ &\quad + \int_0^{2\pi} \int_{\epsilon}^R E(r, \theta) \frac{\alpha_i^M(r) \alpha_k^M(r)}{r^2} \left[ \frac{d}{d\theta} \beta_j^N(\theta) \right] \left[ \frac{d}{d\theta} \beta_\ell^N(\theta) \right] r dr d\theta. \end{aligned} \quad (16)$$

$$F_{k\ell}^{MN} = \int_0^{2\pi} \int_{\epsilon}^R f(r, \theta) \alpha_k^M(r) \beta_\ell^N(\theta) r dr d\theta, \quad (17)$$

and

$$G_{kl}^{MN} = \int_0^{2\pi} \int_{\epsilon}^R E(r, \theta) \hat{k} \beta_l^N(\theta) \left[ \frac{d}{dr} \alpha_k^M(r) \right] r dr d\theta. \quad (18)$$

We note here that

$$K_{kl,ij}^{MN} = K_{il,kj}^{MN} = K_{kj,il}^{MN} = K_{ij,kl}^{MN}. \quad (19)$$

The system (15) can be written in vector matrix notation as

$$A^{MN} w^{MN} = c^{MN} \quad (20)$$

where, in partitioned matrix form,

$$A^{MN} = (A_{pq}^{MN}), \quad (p = 1, \dots, M-1; \quad q = 1, \dots, M-1) \quad (21)$$

and, for fixed p and q,

$$A_{pq}^{MN} = (K_{pi,qj}^{MN}) \quad (22)$$

for (row)  $i = 1, \dots, N$ , and (column)  $j = 1, \dots, N$ . From properties (19), we also have that

$$A_{pq}^{MN} = [A_{pq}^{MN}]^T = A_{qp}^{MN}. \quad (23)$$

In addition, the vectors  $w^{MN}$  and  $c^{MN}$  are given by

$$w^{MN} = \begin{bmatrix} w_{11}^{MN} \\ w_{12}^{MN} \\ \vdots \\ \vdots \\ w_{1N}^{MN} \\ \\ w_{21}^{MN} \\ w_{22}^{MN} \\ \vdots \\ \vdots \\ w_{2N}^{MN} \\ \\ \vdots \\ \vdots \\ w_{M-1,1}^{MN} \\ w_{M-1,2}^{MN} \\ \vdots \\ \vdots \\ w_{M-1,N}^{MN} \end{bmatrix} \quad (24)$$

and

$$c^{MN} = \begin{bmatrix} F_{11}^{MN} + G_{11}^{MN} \\ F_{12}^{MN} + G_{12}^{MN} \\ \vdots \\ F_{1N}^{MN} + G_{1N}^{MN} \\ \\ F_{21}^{MN} + G_{21}^{MN} \\ F_{22}^{MN} + G_{22}^{MN} \\ \vdots \\ F_{2N}^{MN} + G_{2N}^{MN} \\ \\ \vdots \\ \\ F_{M-1,1}^{MN} + G_{M-1,1}^{MN} \\ F_{M-1,2}^{MN} + G_{M-1,2}^{MN} \\ \vdots \\ F_{M-1,N}^{MN} + G_{M-1,N}^{MN} \end{bmatrix} \quad (25)$$

For large values of the product  $MN$ ,  $A^{MN}$  is high order,  $((M-1)N \times (M-1)N)$ . It is a symmetric, sparse matrix which can be partitioned as  $(M-1)^2 \times N$  submatrices. Sparse matrix techniques can be avoided in solving (20) if we assume that  $E(r, e)$  is separable. That is,

$$E(r, \theta) = E_1(r) E_2(\theta) \quad (26)$$

where  $E_1(r) > 0$  and  $E_2(\theta) > 0$ ; we may now write

$$K_{pi,qj}^{MN} = a_{ji}^N b_{qp}^M + c_{ji}^N d_{qp}^M \quad (27)$$

where

$$a_{ji}^N = a_{ij}^N = \int_0^{2\pi} E_2(\theta) \beta_j^N(\theta) \beta_i^N(\theta) d\theta, \quad (28)$$

$$b_{qp}^M = b_{pq}^M = \int_{\epsilon}^R E_1(r) \left[ \frac{d}{dr} \alpha_q^M(r) \right] \left[ \frac{d}{dr} \alpha_p^M(r) \right] r dr, \quad (29)$$

$$c_{ji}^N = c_{ij}^N = \int_0^{2\pi} E_2(\theta) \left[ \frac{d}{d\theta} \beta_j^N(\theta) \right] \left[ \frac{d}{d\theta} \beta_i^N(\theta) \right] d\theta \quad (30)$$

and

$$d_{qp}^M = d_{pq}^M = \int_{\epsilon}^R E_1(r) \frac{\alpha_q^M(r) \alpha_p^M(r)}{r} dr. \quad (31)$$

Utilizing (27) and defining matrices

$$\mathbf{A}^N = (a_{ij}^N) \quad (i = 1, \dots, N; j = 1, \dots, N), \quad (32)$$

$$\mathbf{B}^M = (b_{qp}^M) \quad (q = 1, \dots, M-1; p = 1, \dots, M-1), \quad (33)$$

$$\mathbf{C}^N = (c_{ij}^N) \quad (i = 1, \dots, N; j = 1, \dots, N), \quad (34)$$

$$\mathbf{D}^M = (d_{pq}^M) \quad (p = 1, \dots, M-1; q = 1, \dots, M-1), \quad (35)$$

we are able to rewrite (21) and (22) as

$$A_{pq}^{MN} = b_{qp}^M \tilde{A}^N + d_{pq}^M \tilde{C}^N, \quad (36)$$

$$A^{MN} = \tilde{B}^M \otimes \tilde{A}^N + \tilde{D}^M \otimes \tilde{C}^N \quad (37)$$

where the symbol  $\otimes$  denotes matrix direct product [21].

Equation (20) now becomes

$$[\tilde{B}^M \otimes \tilde{A}^N + \tilde{D}^M \otimes \tilde{C}^N]w^{MN} = c^{MN} \quad (38)$$

which is equivalent [21, p. 261] to the matrix equation

$$\tilde{B}^M w^{MN} \tilde{A}^N + \tilde{D}^M w^{MN} \tilde{C}^N = \tilde{E}^{MN} \quad (39)$$

where

$$w^{MN} = (w_{ij}^{MN}) \quad (i = 1, \dots, M-1; \quad j = 1, \dots, N) \quad (40)$$

and

$$\tilde{E}^{MN} = (F_{ij}^{MN} + G_{ij}^{MN}) \quad (i = 1, \dots, M-1; \quad j = 1, \dots, N) . \quad (41)$$

The coefficient matrices of  $w^{MN}$  in (39) have numerically attractive properties:

- (i) all are symmetric, (ii)  $\tilde{B}^M$ ,  $\tilde{C}^N$ , and  $\tilde{D}^M$  are banded (tri-diagonal), and
- (iii)  $\tilde{A}^N$  and  $\tilde{D}^M$  are positive definite.

Research to construct a numerical algorithm for solving (39) which utilizes these properties is planned. At present, (39) is rewritten in the equivalent form

$$[(\tilde{D}^M)^{-1} \tilde{B}^M]w^{MN} + w^{MN} [\tilde{C}^N (\tilde{A}^N)^{-1}] = (\tilde{D}^M)^{-1} \tilde{E}^{MN} (\tilde{A}^N)^{-1} \quad (42)$$

and solved by the Bartels-Stewart algorithm [22].

In order to estimate, via a numerical scheme, the functional coefficients  $E_1$  and  $E_2$ , we must further parametrize these functions so that identification is performed over a finite-dimensional (instead of an infinite-dimensional) parameter set. Our approach here is to consider a spline-based representation for each so that the shape of  $E_1$ ,  $E_2$  is not assumed in advance (as would be the case if  $E_1$ ,  $E_2$  were assumed to be affine functions, for example). To this end, we let

$$E_1(r) = \sum_{k=1}^{M_1} v_k \lambda_k(r) \quad (43)$$

$$E_2(\theta) = \sum_{j=1}^{N_1} \delta_j \mu_j(\theta) \quad (44)$$

where  $v_k$  and  $\delta_j$  are scalar parameters and  $\lambda_k$  and  $\mu_j$  are cubic B-spline functions defined [20, p. 61] over  $[\epsilon, R]$  and  $[0, 2\pi]$ , respectively, whose orders are independent of  $M$  and  $N$ . The functions have been modified so that  $\mu_j$  satisfies periodic boundary conditions. Using (43) and (44),

$$\tilde{A}^N = \sum_{k=1}^{N_1} \delta_k \tilde{A}_k^N \quad (45)$$

$$\tilde{B}^M = \sum_{k=1}^{M_1} v_k \tilde{B}_k^M \quad (46)$$

$$\tilde{C}^N = \sum_{k=1}^{N_1} \delta_k \tilde{C}_k^N \quad (47)$$

$$\tilde{D}^M = \sum_{k=1}^{M_1} v_k \tilde{D}_k^M \quad (48)$$

where the following matrices have been defined:

$$\tilde{A}_k^N = \left( \int_0^{2\pi} \mu_k(\theta) \beta_p^N(\theta) \beta_q^N(\theta) d\theta \right) \quad (p = 1, \dots, N; \quad q = 1, \dots, N) \quad (49)$$

$$\tilde{B}_k^M = \left( \int_{\epsilon}^R \lambda_k(r) \left[ \frac{d}{dr} \alpha_p^M(r) \right] \left[ \frac{d}{dr} \alpha_q^M(r) \right] r dr \right) \quad (p = 1, \dots, M-1; \quad q = 1, \dots, M-1) \quad (50)$$

$$\tilde{C}_k^N = \left( \int_0^{2\pi} \mu_k(\theta) \left[ \frac{d}{d\theta} \beta_p^N(\theta) \right] \left[ \frac{d}{d\theta} \beta_q^N(\theta) \right] d\theta \right) \quad (p = 1, \dots, N; \quad q = 1, \dots, N) \quad (51)$$

$$\tilde{D}_k^M = \left( \int_{\epsilon}^R \lambda_k(r) \frac{\alpha_p^M(r) \alpha_q^M(r)}{r} dr \right) \quad (p = 1, \dots, M-1; \quad q = 1, \dots, M-1). \quad (52)$$

We also obtain, using (43) and (44) to characterize representations for  $E_1$  and  $E_2$ ,

$$\begin{aligned} \tilde{E}_{ij}^{MN} = & \left( F_{ij}^{MN} + \hat{k} \left[ \sum_{k=1}^{N_1} \delta_k \int_0^{2\pi} \mu_k(\theta) \beta_j^N(\theta) d\theta \right] \right. \\ & \left. \left[ \sum_{k=1}^{M_1} v_k \int_{\epsilon}^R \lambda_k(r) r \frac{d}{dr} \alpha_i^M(r) dr \right] \right) \quad (53) \end{aligned}$$

$$i = 1, \dots, M-1; \quad j = 1, \dots, N).$$

We turn next to implementation of the parameter estimation scheme, i.e., the numerical determination of  $v_k$ ,  $k = 1, \dots, M_1$ , and  $\delta_j$ ,  $j = 1, \dots, N_1$ , that appear in (43) and (44) and correspond to "optimal" values of the parameters  $E_1$  and  $E_2$ .

### V. The Parameter Estimation Algorithm

Appealing to the ideas found in previous sections, we may now detail an algorithm for estimating the coefficients  $v_k$ ,  $k = 1, \dots, M_1$ , and  $\delta_j$ ,  $j = 1, \dots, N_1$ , for  $E(r, \theta)$  that provide the "best fit" between approximations for the state  $u$  and observed data  $u_m$  obtained from various sample points on the surface. We may equivalently consider data for  $y$  by making the transformation

$$y_m(r_i, \theta_j) = u_m(r_i, \theta_j) - \left( \frac{r_i - R}{\epsilon - R} \right) u_0 \quad (54)$$

for  $i = 1, \dots, L_r$ , and  $j = 1, \dots, L_\theta$ .

We organize the parameter estimation algorithm into the following steps.

1. Select an order of approximation for the cubic spline elements  $\lambda_k$ ,  $k = 1, \dots, M_1$ , and  $\mu_j$ ,  $j = 1, \dots, N_1$ , used to represent  $E_1$  and  $E_2$ . Set  $n = 1$ .
2. Select  $M$  and  $N$ , the orders of the linear spline basis elements used to represent  $u^{M,N}$  (and  $y^{M,N}$ ).
3. Assume a nominal set of values for

$$v = (v_1, v_2, \dots, v_{M_1}) \quad (55)$$

and

$$\delta = (\delta_1, \delta_2, \dots, \delta_{N_1}) \quad (56)$$

4. Calculate the coefficient matrices in (42) and solve for  $W^{MN}(\nu, \delta)$ .
5. Calculate, from (14),  $y_i^{M,N}(r_i, \theta_j; \nu, \delta)$  and evaluate

$$J^{MN}(\nu, \delta) = \sum_{i=1}^{L_r} \sum_{j=1}^{L_\theta} [y_i^{M,N}(r_i, \theta_j; \nu, \delta) - y_m(r_i, \theta_j)]^2. \quad (57)$$

6. Proceed to step 8 if  $J^{M,N}(\nu, \delta)$  is sufficiently small. Otherwise, through an optimization procedure, determine a new pair  $(\tilde{\nu}, \tilde{\delta})$  which decreases the value of  $J^{M,N}$ . If no such pair can be found, go to step 8.
7. Set  $(\nu, \delta) = (\tilde{\nu}, \tilde{\delta})$  and return to step 4.
8. Preserve the current values of  $J^{M,N}$  and the corresponding  $(\nu, \delta)$  pair as the  $n^{\text{th}}$  entry in a sequence of these pairs, ordered with increasing  $M$  and  $N$ .
9. Proceed to step 10 if sufficient data has been obtained to analyze the sequences. Otherwise, set  $n = n+1$  and return to step 2 with increased  $M$  and  $N$ . The current values of  $(\nu, \delta)$  will be used as initial values for the next optimization process.
10. From analysis of the numerical sequences, select the  $M, N$  entry which indicates the best numerical results. The corresponding  $(\nu, \delta)$  pair yields  $E(r, \theta)$  which determines the material properties of the antenna mesh. The matrix  $W^{MN}(\nu, \delta)$ , when used in conjunction with (14), determines an approximation  $y^{M,N}$  of the shape of the antenna surface.

For the examples reported in the next section, a Levenberg-Marquardt [23] (Damped Least Squares) nonlinear programming scheme was applied at step 6.

A convergence theory has been developed for our parameter estimation algorithm and will be outlined in section VII below. We instead focus next on a comprehensive discussion of our numerical findings to date.

## VI. Numerical Results

We present here our findings for a number of test examples. In Example 1 and 2 we demonstrate the effectiveness of the scheme outlined in Section V as it is applied to representative model equations. We then turn to Example 3, which is constructed based on proposed physical characteristics of the antenna surface (such specifications are detailed in [16]). Lacking at present actual experimental data from the Hoop/Column antenna, we hope, in this example, to best emulate the type of data expected from the antenna.

For each example, a  $L_r \times L_\theta$  grid  $\{y_m(r_i, \theta_j), i = 1, \dots, L_r, j = 1, \dots, L_\theta\}$  of the data points is generated by choosing a desired shape  $\bar{u}$  and evaluating  $\bar{u}$  (with noise added in some cases) at  $(r_i, \theta_j), i = 1, \dots, L_r, j = 1, \dots, L_\theta$ ; the numerical package is then given the data and the distributed load  $f$ , where  $f$  is calculated by substituting the noise-free  $\bar{u}$  and a choice of elastic parameter  $E$  into equation (1). For desired values of  $N$  and  $M$ , and an initial guess  $E^0$  for  $E$ , we apply standard optimization schemes to minimize  $J^{MN}$  (given in (57)). In each case, we take  $E(r, \theta) = E_1(r)E_2(\theta)$  where we approximate  $E_1$  and  $E_2$  by linear combinations of cubic spline functions in  $r$  and  $\theta$ , respectively. Throughout, equations (43) and (44) are used to represent  $E_1$  and  $E_2$ , using  $M_1 = N_1 = 4$ .

All numerical examples presented here were computed on the CDC 6600 at Southern Methodist University. We would like to express our sincere appreciation to David Krakosky at S.M.U. who assisted in the preparation of data and graphical display of these results. The optimization scheme employed to minimize  $J^{MN}$  is the IMSL version (ZXSSQ) of the Levenberg-Marquardt algorithm, where we typically use default values of IMSL parameters.

For each example reported below, values of  $M$  (or  $N$ ) are specified; in order that  $M-1$  basis elements are used in both  $r$  and  $\theta$  directions, we take  $N = M-1$ . Two measures of performance will be given in each case:  $(J^{MN})^{1/2}$  (which provides a good measure of state approximation) and  $R^{M,N}$  where, using  $|\cdot|$  to denote the  $L_2$  norm on  $[\epsilon, R] \times [0, 2\pi]$ ,

$$R^{M,N} = \frac{|E^{MN} - \bar{E}|}{|\bar{E}|} \times 100\%$$

measures the relative error between the "true" parameter  $\bar{E}$  and the "optimal" parameter  $E^{MN}$  associated with the  $(M,N)$ th approximate parameter estimation problem. We also report CP time which can be reduced considerably by relaxing the convergence criteria for the IMSL package and by taking as initial guesses (for the  $(M,N)$ th problem) the resultant  $E^{MN}$  from an earlier run ( $\tilde{M} < M$ ,  $\tilde{N} < N$ ). This procedure is used in Example 3.

Example 1.1: Here we take  $\epsilon = 1$ ,  $R = 6$ ,  $u_0 = -50$ ,  $\bar{u}(r, \theta) = -(6-r)[(r-1)(\sin(2\theta+2) + 10)]$  and  $\bar{E}(r, \theta) = .25(r-3)^2 + 2$ , for  $1 \leq r \leq 6$  and  $0 \leq \theta \leq 2\pi$ . A  $7 \times 7$  grid of sample data is computed; throughout  $E_2$  is fixed at  $E_2 \equiv 1$  so that we identify  $E_1$  only, starting from an initial guess of  $E_1^0 \equiv .001$ . Our findings are summarized in Table 1 and Figure 3.

Example 1.2: We repeat the same example but now add random noise (distributed normally with mean 0 and variance .75) to the data, resulting in approximately 5% relative error. Numerical and graphical results are found in Table 2 and Figure 4.

Example 1.3: We repeat Example 1.1 (i.e., noise-free data) except that now we estimate  $E_2(\theta)$  as well. We initially set  $E_1^0 \equiv .1$  and  $E_2^0(\theta) = .359(2 - \sin(\frac{\theta}{2}))$  and hold fixed the leading coefficient (in the spline expansion (44)) for  $E_2(\theta)$ . The results for  $M = 25$  are found in Table 3 and Figures 5(a) and (b).

Example 2: In this example, we choose  $u_0 = -24$ ,  $\epsilon = 2$ ,  $R = 6$ ,  $\bar{u}(r, \theta) = -(6-r)[(r-2)(\cos 2\theta + 4) + 6]$  and  $\bar{E}(r, \theta) = (-\frac{2}{3}r + 7)(2 - \frac{1}{2}\sin^2 \theta)$ , for  $r \in [2, 6]$  and  $\theta \in [0, 2\pi]$ . Again a  $7 \times 7$  grid of data is used in the optimization procedure. As an initial guess for  $E(r, \theta) = E_1(r)E_2(\theta)$ , we let  $E_1^0(r)E_2^0(\theta) \equiv 1$  and search for both  $E_1$  and  $E_2$ , holding the first coefficient fixed in the cubic spline representation for  $E_2$ . A summary of our findings for Example 2 may be found in Table 4 below.

### EXAMPLE 1

Table 1: Results for Example 1.1

M	$R^{M,N}$	$(J^{MN})'$	CP time (Sec.)
4	4.75%	19.86	8.52
8	19.64%	3.61	23.97
16	4.66%	0.44	89.43
24	2.25%	0.23	284.03
32	0.68%	0.11	655.49

Table 2: Results for Example 1.2

M	$R^{M,N}$	$(J^{MN})^{\frac{1}{2}}$	CP time (Sec.)
4	21.83%	21.26	6.78
8	18.92%	6.82	20.80
16	4.44%	5.73	104.97
24	2.34%	5.65	410.51
32	1.17%	5.64	815.85

Table 3: Results for Example 1.3

M	$R^{M,N}$	$(J^{MN})^{\frac{1}{2}}$	CP time (Sec.)
25	9.16%	0.17	370.87

Table 4: Results for Example 2

M	$R^{M,N}$	$(J^{MN})^{\frac{1}{2}}$	CP time (Sec.)
4	6.86%	2.40	11.03
8	3.41%	1.58	34.21
16	0.99%	0.38	313.68
24	0.48%	0.10	1200.00

Example 3: We present here our efforts to construct functions  $\bar{u}$  and  $\bar{E}$  that follow many of the specifications of the Hoop/Column antenna surface found in [16].

As shown in Figure 6, the parent reflector has four separate areas of illumination or aperture on its surface. Each separate area is assumed to have the same parabolic shape given, for  $0 \leq \theta \leq \frac{\pi}{2}$  and  $\epsilon \leq r \leq R$ , by

$$u^0(r, \theta) = \begin{cases} \frac{u_0(R-r)}{R-\epsilon} [k(\frac{r-\epsilon}{R}) q_2(\theta) + 1], & 0 \leq \theta \leq \frac{\pi}{36} \\ \frac{u_0(R-r)}{R-\epsilon} [k(\frac{r-\epsilon}{R}) q_1(\theta) + 1], & \frac{\pi}{36} \leq \theta \leq \frac{17\pi}{36} \\ \frac{u_0(R-r)}{R-\epsilon} [k(\frac{r-\epsilon}{R}) q_3(\theta) + 1], & \frac{17\pi}{36} \leq \theta \leq \frac{\pi}{2} \end{cases} \quad (59)$$

where

$$q_1(\theta) = \sin\theta + \cos\theta, \quad (60)$$

$$q_2(\theta) = a_2(\theta - \frac{\pi}{36})^3/6 + \frac{1}{2}(\theta - \frac{\pi}{36})^2 \frac{d^2 q_1}{d\theta^2}(\frac{\pi}{36}) + (\theta - \frac{\pi}{36}) \frac{dq_1}{d\theta}(\frac{\pi}{36}) + q_1(\frac{\pi}{36}), \quad (61)$$

$$a_2 = -\frac{279936}{\pi^3} \left\{ q_1(0) - \frac{\pi^2}{2592} \frac{d^2 q_1}{d\theta^2}(\frac{\pi}{36}) + \frac{\pi}{36} \frac{dq_1}{d\theta}(\frac{\pi}{36}) - q_1(\frac{\pi}{36}) \right\}, \quad (62)$$

$$q_3(\theta) = a_3(\theta - \frac{17\pi}{36})^3/6 + \frac{1}{2}(\theta - \frac{17\pi}{36})^2 \frac{d^2 q_1}{d\theta^2}(\frac{17\pi}{36}) + (\theta - \frac{17\pi}{36}) \frac{dq_1}{d\theta}(\frac{17\pi}{36}) + q_1(\frac{17\pi}{36}), \quad (63)$$

$$a_3 = \frac{279936}{\pi^3} \left\{ q_1 \left( \frac{\pi}{2} \right) - \frac{\pi^2}{2592} \frac{d^2 q_1}{d\theta^2} \left( \frac{17\pi}{36} \right) - \frac{\pi}{36} \frac{dq_1}{d\theta} \left( \frac{17\pi}{36} \right) - q_1 \left( \frac{17\pi}{36} \right) \right\}. \quad (64)$$

The parameter  $k > 0$  is a stretch factor used to perturb the surface below the conic ( $k = 0$ ) shape.

For the complete surface, we define, for  $\epsilon \leq r \leq R$ ,

$$\bar{u}(r, \theta) = \begin{cases} u^0(r, \theta) & 0 \leq \theta \leq \frac{\pi}{2} \\ u^0(r, \theta - \frac{\pi}{2}), & \frac{\pi}{2} \leq \theta \leq \pi \\ u^0(r, \theta - \pi), & \pi \leq \theta \leq \frac{3\pi}{2} \\ u^0(r, \theta - \frac{3\pi}{2}), & \frac{3\pi}{2} \leq \theta \leq 2\pi \end{cases}. \quad (65)$$

The cubic polynomial fits (61) and (63) are used to ensure smoothness in  $\theta$ , in regions near  $\theta = \frac{\pi}{2}, \pi, \frac{3\pi}{2}, 2\pi$ .

We turn now to equations for  $\bar{E}(r, \theta) = \bar{E}_1(r)\bar{E}_2(\theta)$ . It is expected that the mesh will be stiffest near the outer hoop ( $r = R$ ) and around the inner radius ( $r = \epsilon$ ). For this reason we choose

$$\bar{E}_1(r) = 2\tau - \hat{\tau} \sin\left[\pi \frac{(r-\epsilon)}{(R-\epsilon)}\right] \quad (\epsilon \leq r \leq R) \quad (66)$$

where  $\hat{\tau}$  is a constant dependent on the mesh material. Stiffness in the angular direction is expected to be uniform, given here by

$$\bar{E}_2(\theta) = \hat{\tau}. \quad (67)$$

From data provided in [16], it appears that a reasonable value for  $\hat{\tau}$  (given in units  $\sqrt{N/m}$ ) is

$$\hat{\tau} = 3.391 ; \quad (68)$$

similarly, other parameters are estimated to be  $u_0 = -7.5 \text{ m}$ ,  $\epsilon = 8.235 \text{ m}$ , and  $R = 50 \text{ m}$ . For the example reported here, we take  $k = .25$ .

For each example below, a  $24 \times 24$  grid of data points is calculated by determining  $\bar{u}$  at  $(r_i, \theta_j)$  where  $\theta_j$  are equally spaced in  $[0, 2\pi]$ ,  $j = 1, \dots, 24$ , and the  $r_i$  are spaced in a non-uniform manner, with more data points concentrated near  $r = R$ .

Example 3.1: In an effort to determine how well the state approximation scheme performs when  $E$  is fixed at the "true" value  $E = \bar{E}$ , we solved the "forward" problem initially to assess what values of  $J^{MN}$  to expect in later "inverse" problem runs. To this end, we compare in Table 5 below  $J^{MN}$  for various values of  $M$  ( $N = M-1$ ). To interpret Table 5, it is helpful to calculate the average error at each of the 576 sampling locations: In the case of  $M = 4$  we compute the average difference  $|\bar{u}(r_i, \theta_j) - u^{M,N}(r_i, \theta_j)| = (J^{MN}/576)^{1/2} = .056$ .

Table 5: Example 3.1

N	$(J^{MN})^{1/2}$
4	1.82
8	1.88
16	1.92
24	1.94
30	1.94

We note that a little reflection leads to the conclusion that the values of  $J$  reported in Table 5 are not lower bounds for the values of  $J$  obtained in

the minimization procedures detailed below (here we are using the approximate states and a spline approximation to the "true"  $E$ ). This is evident in the subsequent tables for this example.

Example 3.2: We estimate  $E_1(r)$  only, holding  $E_2(\theta)$  fixed at the true value,  $\bar{E}_2(\theta)$ . For each  $M$ , the initial guess for  $E_1$  is  $E_1^0(r) \equiv 1$ . Our results are summarized in Table 6, and graphs comparing  $E_1^{MN}$  to  $\bar{E}_1$  are found in Figure 7.

Example 3.3: We now hold  $E_1(r)$  fixed,  $E_1(r) \equiv \bar{E}_1(r)$ , and estimate  $E_2$  from the starting guess of  $E_2^0(\theta) = 1 + .5 \cos \theta$  (in the case of  $N = 4$ ). For  $N = 8, 16, 24$ , and  $30$ , we use the earlier converged value of  $E^{MN}$  as the initial guess (e.g.,  $E_2^0$  for  $N = 8$  is  $\tilde{E}_2^{MN}$ ,  $N = 4$ ). Findings for this example are summarized in Table 7; graphs of  $E_2^{MN}$ , plotted against  $\bar{E}_2$ , may be found in Figure 8.

Example 3.4: We estimate both  $E_1(r)$  and  $E_2(\theta)$ . Initial guesses for  $N = 4$  are given by  $E_1^0(r) = 5$  and  $E_2^0(\theta) = 1 - \frac{1}{4} \sin \theta$ ; for  $N = 8, 16, 24$ , and  $30$ , previous estimates ( $E_1^{MN}, E_2^{MN}$ ) are used. In each case, the first coefficient for  $E_2$  is held fixed. The convergence results for this example may be found in Table 8.

Example 3.5: This example is identical to that of Example 3.2, except that random noise has been added to the data. The new data  $\hat{u}(r_i, \theta_j)$  is computed by setting

$$\hat{u}(r_i, \theta_j) = n_{ij} \cdot \sigma_k(r_i, \theta_j) + \bar{u}(r_i, \theta_j)$$

where  $n_{ij}$  is a zero mean normally distributed random number with unit variance and

$$\sigma(r_i, \theta_j) = .025 |\bar{u}(r_i, \theta_j)| .$$

## EXAMPLE 3

ORIGINAL PAGE IS  
OF POOR QUALITY

Table 6: Example 3.2

N	$R^{M,N}$	$(J^{MN})^{\frac{1}{2}}$	CP time (Sec.)
4	37.38%	0.904	25.06
8	7.50%	0.679	33.73
16	4.06%	0.678	168.08
24	4.64%	0.668	226.67
30	4.87%	0.675	440.79

Table 7: Example 3.3

N	$R^{M,N}$	$(J^{MN})^{\frac{1}{2}}$	CP time (Sec.)
4	7.74%	0.983	14.37
8	6.20%	0.763	19.31
16	6.24%	0.763	56.40
24	6.26%	0.758	73.68
30	6.25%	0.765	133.07

Table 8: Example 3.4

N	$R^{M,N}$	$(J^{MN})^{\frac{1}{2}}$	CP time (Sec.)
4	43.27%	0.903	26.88
8	5.67%	0.635	127.31
16	5.78%	0.636	129.81
24	6.60%	0.627	139.19
30	7.00%	0.634	378.21

Thus, with probability of .95, the new data will satisfy

$$\frac{|\hat{u}(r_i, \theta_j) - \bar{u}(r_i, \theta_j)|}{|\bar{u}(r_i, \theta_j)|} \leq .05$$

so that data with, roughly, 5% noise level is used here.

We take  $E_1^0 \equiv 1.0$  for  $N = 4$  and  $8$ , and previous estimates are used as initial guesses for  $N = 16, 24$ , and  $30$ . Graphical representations of  $E_1^{MN}$  vs  $\bar{E}_1$  are found in Figure 9; our findings are summarized in Table 9.

Table 9: Example 3.5

N	$R^{M,N}$	$(J^{MN})^{1/2}$	CP time (Sec.)
4	148.86%	2.669	41.57
8	5.05%	2.616	46.73
16	6.76%	2.612	45.72
24	4.99%	2.610	169.22
30	5.33%	2.611	255.90

## VII. Theoretical Convergence Results

We present here a theoretical framework for the approximation scheme outlined in Section IV. We shall first formulate the variational equation of state and investigate some of its properties; spline-based approximating equations (based on either linear or cubic spline elements) will then be constructed so that we may argue the convergence of approximate states and parameters to the "true" state and "optimal" value of the unknown parameter.

Appealing to the notation of Section II, we may write the total energy of the antenna surface as

$$\mathcal{E}(u) = \iint_{\tilde{\Omega}} \left( \frac{1}{2} E |\nabla u|^2 - uf \right) d\tilde{\Omega}$$

where the elastic coefficient  $E$  and distributed loading  $f$  are written in terms of Cartesian coordinates in  $\tilde{\Omega} = \{(x_1, x_2) \in \mathbb{R}^2 \mid \varepsilon^2 < x_1^2 + x_2^2 < R^2\}$  and

$u \in H_B^1(\tilde{\Omega}) \equiv \{u \in H^1(\tilde{\Omega}) \mid u = y + U, y \in H_0^1(\tilde{\Omega})\}$ ; here

$$U(x_1, x_2) = \frac{u_0}{\varepsilon - R} ((x_1^2 + x_2^2)^{\frac{1}{2}} - R), \quad (x_1, x_2) \in \tilde{\Omega}. \quad (69)$$

From minimum energy considerations, we know that the state variable  $u$  is a stationary point of  $\mathcal{E}$ . That is,  $\mathcal{E}'(u; v) = 0$  for all  $v \in H_0^1(\tilde{\Omega})$ , where  $\mathcal{E}'$  denotes the Frechet derivative of  $\mathcal{E}$ . We thus write, for any  $v \in H_0^1(\tilde{\Omega})$ ,

$$0 = \mathcal{E}'(u; v)$$

$$= \iint_{\tilde{\Omega}} \{E \nabla u \cdot \nabla v - fv\} d\tilde{\Omega},$$

which yields the state equation for  $u \in H_B^1(\tilde{\Omega})$ ,

$$\tilde{a}_E(u, v) = \langle f, v \rangle, \quad v \in H_0^1(\tilde{\Omega}). \quad (70)$$

Here  $\langle \cdot, \cdot \rangle$  is the usual  $L_2(\tilde{\Omega})$  inner product and

$$\tilde{a}_E(u, v) = \iint_{\tilde{\Omega}} E \nabla u \cdot \nabla v \, d\tilde{\Omega}.$$

We remark that if  $u$  and  $E$  are sufficiently smooth, we actually may use Green's Theorem, ([27], p. 342)

$$\iint_{\tilde{\Omega}} E \nabla \phi \cdot \nabla \psi = \int_{\partial \tilde{\Omega}} E \phi \frac{\partial \psi}{\partial n} \, ds - \iint_{\tilde{\Omega}} \phi \nabla \cdot (E \nabla \psi)$$

(for  $\phi \in H^1$ ,  $\psi \in H^2$ ) to rewrite (70) as

$$- \iint_{\tilde{\Omega}} v \nabla \cdot (E \nabla u) \, d\tilde{\Omega} = \iint_{\tilde{\Omega}} v f \, d\tilde{\Omega}$$

since  $v \in H_0^1(\tilde{\Omega})$ . Thus, for sufficiently smooth  $E$  and  $u$ , the state equation in  $u$  becomes Poisson's Equation with variable coefficient,

$$- \nabla \cdot (E \nabla u) = f \text{ on } \tilde{\Omega}. \quad (71)$$

Before we consider various properties of the state equation (70), it is natural to first transform the state variable  $u$  into a new variable  $y$  satisfying homogeneous boundary conditions. To this end we define

$$y = u - U$$

and note that equation (70) may be rewritten in terms of  $y$ ,  $v \in H_0^1(\tilde{\Omega})$  as

$$\tilde{a}_E(y, v) = \langle f, v \rangle - \tilde{a}_E(U, v); \quad (72)$$

further, if  $E \in H^1(\Omega)$  an integration by parts yields

$$\tilde{a}_E(y, v) = \langle F, v \rangle \quad (73)$$

where  $F = f + \nabla \cdot (E \nabla U)$ .

Throughout we shall assume that  $f \in L_2(\Omega)$  and  $E \in Q_1$ , where the set  $Q_1$  is a given set satisfying

$$Q_1 \subseteq \{E \in C^1(\Omega) \mid 0 < m \leq E(x) \leq M, \quad |E|_1 \leq M\}.$$

These conditions on  $E$  ensure that, for any  $y \in H_0^1(\Omega)$ ,

$$m|y|_1^2 \leq \tilde{a}_E(y, y) \leq M|y|_1^2 \quad (74)$$

( $|\cdot|_j$  denotes the usual  $H^j(\Omega)$  norm) so that we may apply Theorem 6, p. 295 of [24], to state the following existence theorem.

Theorem 1: There exists a unique solution  $u \in H_B^1(\Omega)$  to the generalized Dirichlet problem (70) (and thus there exists a unique solution  $y \in H_0^1(\Omega)$  to (72)).

In addition, we obtain the following regularity result, for  $E, f$  sufficiently smooth.

Corollary 1: Let  $E \in Q_1$  and  $f \in L_2(\Omega)$ . The solution  $y$  to (72) satisfies  $y \in H^2(\Omega)$  and

$$|y|_2 \leq c_0(|f| + |E|_1 + |y|) \quad (75)$$

for some constant  $c_0$ . If, in addition,  $f \in H^2$  and  $E \in C^3$ , then  $y \in H^4(\Omega)$  and, for some constant  $c_1$ ,

$$|y|_4 \leq c_1(|f|_2 + |E|_3 + |y|) . \quad (76)$$

Proof: Theorem 17.2, p. 67, of [25] may be applied to (73) to obtain

$$\begin{aligned}|y|_{2+j} &\leq c(|F|_j + |y|) \\ &\leq c(|f|_j + |\nabla \cdot (E \nabla U)|_j + |y|)\end{aligned}$$

for  $j = 0, 2$ , and some constant  $c$ , from which (75) and (76) follow.

Clearly, statements analogous to (75), (76) may be made for the solution  $u$  to (70) since  $u = y + U$ . In fact, although all results reported below involve  $y$ , it is easy to see that the same findings hold for  $u$ . We first establish some a priori bounds for  $y$ .

Lemma 1: Let  $E \in Q_1$ ,  $f \in F_1$ ,  $F_1$  bounded in  $L_2(\Omega)$ , and let  $y$  be the solution to (72). There exist constants  $K_0$ ,  $K_1$  (depending on  $Q_1$  and  $F_1$  only) such that

$$|y(E, f)| \leq K_0 \quad (77)$$

and

$$|\nabla y(E, f)| \leq K_1 \quad (78)$$

uniformly in  $E \in Q_1$ ,  $f \in F_1$ .

Proof: For  $v \in H_0^1$  and  $y = y(E, f)$ ,

$$|\tilde{a}_E(y, v)| \leq |F| |v|$$

so that, letting  $y = v$ ,

$$m |\nabla y|^2 \leq \tilde{a}_E(y, y)$$

$$\leq |F| |y|$$

where  $|F|$  is bounded uniformly in  $E \in Q_1$  and  $f \in F_1$ . It thus follows that

$$|\nabla y|^2 \leq k_0 |y| \quad (79)$$

for some constant  $k_0$  and, applying Poincaré's inequality (given by

$$|y| \leq k_1 |\nabla y| \quad (80)$$

for some constant  $k_1$  and  $y \in H_0^1$ ; see for example, pp. 158-159 of [26]) we obtain (78),

$$|\nabla y| \leq k_0 k_1 \equiv K_1.$$

Combining (80) and (78), inequality (77) also obtains, where  $K_0$  and  $K_1$  are determined independently of  $f \in F_1$ ,  $E \in Q_1$ .

We turn now to the problem of approximating the state variable  $y$  for given values of  $E$  and  $f$ . As our goal is to build a parameter estimation scheme based on linear or cubic spline approximations for the state, we first transform the domain  $\tilde{\Omega}$  into a new domain  $\Omega$  where spline basis elements are more easily constructed. In this case it is natural to transform from Cartesian to polar coordinates so that  $\Omega$  is the rectangle  $(\varepsilon, R) \times (0, 2\pi)$ ; spline elements are easily defined on  $\Omega$ , whereas on  $\tilde{\Omega}$  one must handle the problem of defining such elements on the circular boundary of the annulus.

We transform from Cartesian to polar coordinates in the usual way; appealing to Theorem 3.35, p. 63 of [26], we note that properties of this transformation guarantee the existence of a bounded operator  $T: H^1(\tilde{\Omega}) \rightarrow H^1(\Omega)$  that is merely the composition map

$$(Ty)(r, \theta) = y(\phi(x_1, x_2)) \quad (81)$$

where  $\phi: \tilde{\Omega} \rightarrow \Omega$  is the Cartesian to polar coordinate transformation. From [26], we also have that  $T^{-1}$  exists and is bounded. In polar coordinates, the state equation (73) becomes an equation on  $\Omega$ ,

$$a_E(y, v) = \langle F, v \rangle_{\Omega} \quad (82)$$

$$\text{where } a_E(y, v) \equiv \iint_{\Omega} (TE) \nabla(Ty) \cdot \nabla(Tv) d\Omega$$

and  $\langle F, v \rangle_{\Omega} \equiv \iint_{\Omega} (TF) \cdot (Tv) d\Omega$ , ( $d\Omega = r dr d\theta$ ). Henceforth we shall not distinguish between  $\langle \cdot, \cdot \rangle$  and  $\langle \cdot, \cdot \rangle_{\Omega}$  or a vector  $w$  and its transformed form  $Tw$ ; however it should be kept in mind that in (73) both  $y$  and  $v$  are in  $H_0^1(\tilde{\Omega})$  while in (82) the transformed state  $Ty$  and associated vector  $Tv$  are in  $H_{0,\text{per}}^1(\Omega) \equiv TH_0^1(\tilde{\Omega})$ . It is worthwhile to note that for smooth  $y \in H_0^1(\tilde{\Omega})$  (so that we actually have  $y = 0$  on  $\partial\tilde{\Omega}$ ), the transformed  $y \in H_{0,\text{per}}^1(\Omega)$  satisfies  $y(\epsilon, \theta) = y(R, \theta) = 0$  and the periodic condition  $y(r, 0) = y(r, 2\pi)$ ,  $(r, \theta) \in \Omega$ . In addition, we remark that the gradient operator  $\nabla$  in (82) is the polar coordinate transformation of the usual gradient in Cartesian coordinates; that is, in (82),

$$\nabla w \equiv \begin{pmatrix} w_r \cos \theta & -\frac{1}{r} w_{\theta} \sin \theta \\ w_r \sin \theta & +\frac{1}{r} w_{\theta} \cos \theta \end{pmatrix} \quad (83)$$

for  $w \in H^1(\Omega)$ . It is interesting to note that although  $\nabla$  in (83) is the correct form of the gradient in polar coordinates, one often sees in the literature the operator  $\tilde{\nabla}$  given by

$$\tilde{\nabla} w \equiv \begin{pmatrix} w_r \\ \frac{1}{r} w_{\theta} \end{pmatrix} . \quad (84)$$

In fact  $\nabla$  and  $\bar{\nabla}$  may be used interchangeably in some circumstances (and indeed the latter greatly simplifies calculations), largely due to the fact that

$$\nabla w \cdot \nabla z = \bar{\nabla} w \cdot \bar{\nabla} z \quad (85)$$

and

$$\nabla \cdot \nabla w = \nabla \cdot \bar{\nabla} w = \Delta w \quad (86)$$

for  $w, z \in H^1(\Omega)$ . One must be careful however to use  $\nabla$ , and not  $\bar{\nabla}$ , in cases involving an integration by parts (Green's formula).

We turn now to spline-based approximation for the state variable  $y$  in (82). For positive integers  $M$  and  $N$  we subdivide  $[\epsilon, R]$  and  $[0, 2\pi]$  by defining partition points  $r_i^M = \epsilon + (R-\epsilon)(i-1)/M$ ,  $i = 1, \dots, M+1$ , and  $\theta_j^N = 2\pi(j-1)/N$ ,  $j = 1, \dots, N+1$ . We then construct a  $k$ -th order spline approximation  $y_k^{M,N}$  for  $y$  using Galerkin techniques. That is, we find  $y_k^{M,N} \in S_k^{M,N} = \text{span} \{v_{k,ij}^{M,N}\}$ ,  $i = 1, \dots, M_1$ ,  $j = 1, \dots, N_1\}$  where the basis elements  $v_{k,ij}^{M,N}$  are tensor products of the  $k$ -th order spline elements,

$$v_{k,ij}^{M,N}(r, \theta) = \alpha_{k,i}^M(r) \beta_{k,j}^N(\theta); \quad (87)$$

both  $\alpha_{k,i}^M$  and  $\beta_{k,j}^N$  are standard  $k$ -th order B-spline elements that have been modified to match the  $H_{0,\text{per}}^1(\Omega)$  boundary conditions. That is,

$$\alpha_{k,i}^M(\epsilon) = \alpha_{k,i}^M(R) = 0, \quad \text{all } i,$$

and

$$\beta_{k,j}^N(0) = \beta_{k,j}^N(2\pi), \quad \text{all } j.$$

We remark here that the dimension of  $S_k^{M,N}$  depends on  $k$  as well as on  $M$  and  $N$ ; in the case of linear splines ( $k = 1$ ),  $M_1 = M - 1$  and  $N_1 = N$ .

To approximate the solution  $y$  to (82) for fixed  $k$  and  $E \in Q_1$ ,  $f \in F_1$  given, we look for a solution  $y_k^{M,N}$  in  $S_k^{M,N}$  to the Galerkin equations,

$$a_E(y_k^{M,N}, v_{k,ij}^{M,N}) = \langle F, v_{k,ij}^{M,N} \rangle \quad (88)$$

for  $i = 1, \dots, M_1$  and  $j = 1, \dots, N_1$ . In the case of linear splines ( $k = 1$ ), substitution of (87) into (88) yields the algebraic equations found in (15) of Section IV. There is no difficulty in establishing existence and uniqueness of solutions to (88) given the properties of the inner product matrices that appear in the algebraic equations derived from (88).

Our goal is to construct a sequence of parameters  $(\bar{E}^{M,N}, \bar{f}^{M,N}) \in Q_1 \times F_1$  and associated solutions  $y_k^{M,N}(\bar{E}^{M,N}, \bar{f}^{M,N})$  to (88) and determine that  $(\bar{E}^{M,N}, \bar{f}^{M,N}) \rightarrow (\bar{E}, \bar{f})$  and  $y_k^{M,N}(\bar{E}^{M,N}, \bar{f}^{M,N}) \rightarrow y(\bar{E}, \bar{f})$  in some sense; here  $(\bar{E}, \bar{f})$  is an "optimal" parameter vector in the sense that it minimizes a distributed least squares fit-to-data criterion of the form

$$J(E, f) = \iint_{\Omega} |y(E, f) - y_m|^2 d\Omega,$$

where  $y_m$  is the interpolated form of the pointwise data (transformed to satisfy homogeneous boundary conditions, as defined in (54)). If we use the form of the cost functional given in (57) we must strengthen the convergence results given in this section which can be done, but at the expense of additional technical tedium. Given pointwise data, we can use the  $J$  just defined if we interpolate this data. The minimization of the cost functional is performed over some constraint set  $Q \times F$ . In the case of linear splines, we choose

$Q \times F = Q_1 \times F_1$  and, as later results will show, we do obtain the desired parameter and state variable convergence as  $M, N \rightarrow \infty$ . If, instead, cubic splines are to be used, convergence results are obtained at the expense of the requirement that  $Q$  and  $F$  be smoother sets. In particular, we need  $Q = Q_3$  and  $F = F_3$  where, for  $p = 2, 3$ ,

$$Q_p \equiv \{E \in C^p(\Omega) \mid E \in Q_1, |E|_p \leq m\}$$

$$F_p \equiv \{f \in H^{p-1}(\Omega) \mid f \in F_1, |f|_{p-1} \leq m\}.$$

Before considering parameter and state convergence, we establish the continuous dependence of  $y$ ,  $y_k^{M,N}$  on the parameters  $E$  and  $f$ .

Lemma 2: Let  $k = 1$  or  $3$ .

- (a) The mapping  $(E, f) \rightarrow y_k^{M,N}(E, f) : Q_1 \times F_1 \rightarrow H_0^1(\Omega)$  is continuous in the  $L_2 \times L_2$  topology on  $Q_1 \times F_1$ .
- (b) The mapping  $(E, f) \rightarrow y(E, f) : Q_1 \times F_1 \rightarrow H_0^1(\Omega)$  is continuous in the  $L_\infty \times L_2$  topology on  $Q_1 \times F_1$ . At  $(\hat{E}, \hat{f}) \in Q_2 \times F_2$ ,  $y$  is continuous in the  $L_2 \times L_2$  topology on  $Q_1 \times F_1$ .

Proof: We first consider the continuity of  $(E, f) \rightarrow y(E, f)$ . Let  $E, \hat{E} \in Q_1$ ,  $f, \hat{f} \in F_1$  and let  $y = y(E, f)$ ,  $\hat{y} = y(\hat{E}, \hat{f})$ . Then,

$$\begin{aligned} \iint_{\Omega} E \nabla(y - \hat{y}) \cdot \nabla v d\Omega &= \iint_{\Omega} (\hat{E} - E) \nabla y \cdot \nabla v d\Omega + \iint_{\Omega} (E \nabla y - \hat{E} \nabla \hat{y}) \cdot \nabla v d\Omega \\ &= \iint_{\Omega} (\hat{E} - E) \nabla \hat{y} \cdot \nabla v d\Omega + a_E(y, v) - a_{\hat{E}}(\hat{y}, v) \\ &= \iint_{\Omega} (\hat{E} - E) \nabla \hat{y} \cdot \nabla v d\Omega + \langle F, v \rangle - \langle \hat{F}, v \rangle \end{aligned}$$

for all  $v \in H_0^1(\Omega)$  where we have used (82) in the last equality and  $\hat{F} = \hat{f} + \nabla \cdot (\hat{E}\nabla U)$ ,  $F = f + \nabla \cdot (E\nabla U)$ . In particular, if we let  $v = y - \hat{y}$ , we obtain

$$\begin{aligned} \iint_{\Omega} E |\nabla(y - \hat{y})|^2 d\Omega &= \iint_{\Omega} (\hat{E} - E) \nabla \hat{y} \cdot \nabla(y - \hat{y}) d\Omega + \langle f - \hat{f}, y - \hat{y} \rangle \\ &\quad + \langle \nabla \cdot \{(\hat{E} - E)\nabla U\}, y - \hat{y} \rangle . \end{aligned}$$

After an integration by parts and several applications of the Cauchy-Schwarz inequality, we have

$$\begin{aligned} m |\nabla(y - \hat{y})|^2 &\leq |(\hat{E} - E)\nabla \hat{y}| |\nabla(y - \hat{y})| + |f - \hat{f}| |y - \hat{y}| + |(\hat{E} - E)\nabla U| |\nabla(y - \hat{y})| \\ &\leq K_1 |(\hat{E} - E)\nabla \hat{y}| + K_0 |f - \hat{f}| + K_1 |\nabla U|_{\infty} |E - \hat{E}| \end{aligned} \quad (89)$$

where here  $|\cdot|$  denotes the  $L_2(\Omega)$  norm,  $|\cdot|_{\infty}$  denotes the  $L_{\infty}(\Omega)$  norm and  $K_0, K_1$  are given in Lemma 1. Thus

$$|y - \hat{y}|_1^2 \leq c(|(\hat{E} - E)\nabla \hat{y}| + |f - \hat{f}| + |E - \hat{E}|) \quad (90)$$

for some constant  $c > 0$ . For  $(\hat{E}, \hat{f}) \in Q_1 \times F_1$  we have, since  $y \in H^2$ ,

$$\begin{aligned} |y - \hat{y}|_1^2 &\leq c(|\hat{E} - E|_{\infty} |\nabla \hat{y}| + |f - \hat{f}| + \hat{c} |E - \hat{E}|_{\infty}) \\ &\leq c(K_1 |\hat{E} - E|_{\infty} + |f - \hat{f}| + \hat{c} |E - \hat{E}|_{\infty}) , \end{aligned} \quad (91)$$

so that  $(E, f) \mapsto y(E, f)$  is continuous in the  $L_{\infty} \times L_2$  topology. If in addition  $(\hat{E}, \hat{f}) \in Q_2 \times F_2$ , so that  $\hat{y} \in H^3$  (from the proof of Corollary 1), we obtain from the Sobolev Imbedding Theorem (see p. 97, [26])

$$|\hat{y}|_\infty \leq \tilde{c} |\hat{y}|_3$$

where  $|\hat{y}|_3$  is in  $H^3$  because  $(\hat{E}, \hat{f}) \in Q_2 \times F_2$  (again see the proof of Corollary 1). The continuity of  $(E, f) \rightarrow y(E, f)$  at  $(\hat{E}, \hat{f})$  in the  $L_2 \times L_2$  topology is thus assured since (90) may now be rewritten as

$$|y - \hat{y}|_1^2 \leq c(|\hat{E} - E| |\hat{y}|_\infty + |\hat{f} - f| + |E - \hat{E}|). \quad (92)$$

For  $k = 1$  or  $3$ , the continuity of  $(E, f) \rightarrow y_k^{M, N}(E, f)$  in the  $L_2 \times L_2$  topology is apparent from (88). (See, for example, the algebraic equations (15)-(20) in Section IV that replace (88) in the case of  $k = 1$ ; we note that  $|K_{\rho\ell, ij}^{MN}| \leq C|E|$  and  $|F_{\rho\ell}^{MN}| \leq C|f|$  for  $i, \rho = 1, \dots, M-1$  and  $j, \ell = 1, \dots, N$ , where  $C$  is a constant depending on  $M$  and  $N$ . A comparable statement may be made about the matrices involved in the algebraic equations derived for the case of  $k = 3$ .)

Our later convergence arguments rely heavily on certain spline estimates that are simple modifications of those found on pp. 83-84 of [20a]. (In particular, our calculations must take into account the fact that the spline basis elements  $\alpha_{k, i}^M$  on  $[\epsilon, R]$  and  $\beta_{k, j}^N$  on  $[0, 2\pi]$  satisfy zero and periodic boundary conditions respectively. This causes no difficulty since we will only use those elements to approximate functions that satisfy such boundary conditions. For example, in the case of linear splines,  $\{\alpha_i^M\}$  contains all the standard B-spline "hat function" basis elements  $\{\hat{\alpha}_i^M\}$  except the "half-hats",  $\hat{\alpha}_1^M, \hat{\alpha}_{M+1}^M$ . If  $g \in H_0^1(\epsilon, R)$ , then the linear interpolating spline for  $g$  at knots  $\{r_i^M\}$  is given by

$I_L g = \sum_{j=1}^{M+1} \hat{\alpha}_j^M c_j$  where necessarily  $c_1 = c_{M+1} = 0$ . Therefore,  $I_L g = \sum_{j=1}^{M-1} \alpha_j^M c_{j+1}$ . Similarly,  $\{\beta_j^N\}$  contains all the standard B-spline basis elements  $\{\hat{\beta}_j^N\}$  defined on  $[0, 2\pi]$  except that  $\hat{\beta}_1^N$  and  $\hat{\beta}_{N+1}^N$  are combined to form

one element given by  $\beta_N^N = \beta_1^N + \beta_{N+1}^N$ . We thus get, for a  $2\pi$ -periodic function  $g$ ,

$I_L g = \sum_{i=1}^{N+1} \beta_i^N d_i = \sum_{i=2}^{N-1} \beta_i^N d_i + (d_1 + d_{N+1}) \beta_N^N$ . The spline estimates needed for later convergence proofs are given below.

Lemma 3: Let  $\psi \in H^{k+1}(\Omega) \cap H_{0,per}^1(\Omega)$  for  $k = 1$  or  $3$ . If  $P_k^{M,N}$  denotes the canonical projection of  $L_2(\Omega)$  onto  $S_k^{M,N}(\Omega)$  (in the  $L_2(\Omega)$  topology), then

$$|\psi - P_k^{M,N} \psi| \leq C_0(MN)^{-(k+1)} |\mathcal{D}^{k+1} \psi| \quad (93)$$

$$|\mathcal{D}_r(\psi - P_k^{M,N} \psi)| \leq C_1(MN)^{-k} |\mathcal{D}^{k+1} \psi| \quad (94)$$

$$|\mathcal{D}_\theta(\psi - P_k^{M,N} \psi)| \leq C_1(MN)^{-k} |\mathcal{D}^{k+1} \psi|. \quad (95)$$

Finally, we consider the existence of "optimal" parameters  $(\bar{E}, \bar{f})$ , determination of a sequence  $((\bar{E}^{M,N}, \bar{f}^{M,N}))$  of approximating parameters and the convergence, in an appropriate sense, of  $(\bar{E}^{M,N}, \bar{f}^{M,N})$  to  $(\bar{E}, \bar{f})$  and the corresponding state variable convergence, of  $y^{M,N}(\bar{E}^{M,N}, \bar{f}^{M,N})$  to  $y(\bar{E}, \bar{f})$ .

Lemma 4: Let  $Q_1 \times F_1$  be compact in the  $L_2(\Omega) \times L_2(\Omega)$  product topology and let  $k = 1$  or  $3$ . Then there exists a solution  $(\bar{E}^{M,N}, \bar{f}^{M,N}) \in Q_1 \times F_1$  to the problem of minimizing  $J_k^{M,N}$  over  $Q_1 \times F_1$  where

$$J_k^{M,N}(E, f) = \iint_{\Omega} |y_k^{M,N}(E, f) - y_m|^2 d\Omega$$

and  $y_k^{M,N}(E, f)$  is the solution to (88) associated with parameters  $(E, f)$ .

Proof: The result follows immediately from Lemma 2, which guarantees the continuity of  $J_k^{M,N}$  over the compact set  $Q_1 \times F_1$ .

The sense in which  $(\bar{E}^{M,N}, \bar{f}^{M,N})$  approximates  $(\bar{E}, \bar{f})$ , and in turn  $y^{M,N}(\bar{E}^{M,N}, \bar{f}^{M,N})$  approximates  $y(\bar{E}, \bar{f})$ , is given in our final two results.

Theorem 2: Let  $\{(E^{M,N}, f^{M,N})\}$  be a sequence of parameters in  $Q_1 \times \mathcal{F}_1$  and let  $y_k^{M,N}$  be the solution to (88) corresponding to  $E^{M,N}, f^{M,N}$ .

(a) If there exists  $(E, f) \in Q_1 \times \mathcal{F}_1$  such that  $(E^{M,N}, f^{M,N}) \rightarrow (E, f)$  in the  $L_\infty \times L_2$  topology, then  $y_1^{M,N} \rightarrow y(E, f)$  in  $H_0^1(\Omega)$  as  $M, N \rightarrow \infty$ .

(b) Suppose further that  $(E^{M,N}, f^{M,N}) \in Q_1 \times \mathcal{F}_1$ ,  $(E, f) \in Q_2 \times \mathcal{F}_2$  and that  $(E^{M,N}, f^{M,N}) \rightarrow (E, f)$  in the  $L_2 \times L_2$  topology. Then  $y_1^{M,N} \rightarrow y(E, f)$  in  $H_0^1(\Omega)$  as  $M, N \rightarrow \infty$ . If  $(E, f) \in Q_3 \times \mathcal{F}_3$ , then  $y_3^{M,N} \rightarrow y(E, f)$  in  $H_0^1(\Omega)$  as  $M, N \rightarrow \infty$ .

Proof: For parts (a) and (b) it suffices to show that

$$|y_k^{M,N}(E, f) - y(E, f)|_1 \rightarrow 0 \quad \text{as } M, N \rightarrow \infty,$$

uniformly in  $(E, f)$  (in the desired parameter set), because we may then use this result to demonstrate that

$$\begin{aligned} |y_k^{M,N}(E^{M,N}, f^{M,N}) - y(E, f)|_1 &\leq |y_k^{M,N}(E^{M,N}, f^{M,N}) - y(E^{M,N}, f^{M,N})|_1 \\ &\quad + |y(E^{M,N}, f^{M,N}) - y(E, f)|_1 \end{aligned}$$

where both terms converges to zero as  $M, N \rightarrow \infty$ . Here we have used the appropriate continuity result from Lemma 2 to argue the convergence of the second term above.

Let  $(E, f) \in Q_1 \times \mathcal{F}_1$ . For  $k = 1$  or  $3$  we subtract (88) from (82) (with  $v = v_{k,ij}^{M,N} \in H_0^1(\Omega)$ ) to obtain

$$a_E(y(E, f) - y_k^{M, N}(E, f), v_{k, ij}^{M, N}) = 0$$

for  $i = 1, \dots, M_1$ ,  $j = 1, \dots, N_1$ . That is,  $y_k^{M, N}$  is the projection of  $y \in H_0^1$  onto  $S_k^{M, N}$  in the  $a_E(\cdot, \cdot)$  topology (equivalent to the  $H_0^1$  topology). We thus obtain, letting  $y = y(E, f)$ ,  $y_k^{M, N} = y_k^{M, N}(E, f)$ ,

$$\begin{aligned} m|\nabla(y - y_k^{M, N})|^2 &\leq a_E(y - y_k^{M, N}, y - y_k^{M, N}) \\ &\leq a_E(y - P_k^{M, N}y, y - P_k^{M, N}y) \\ &\leq m|\nabla(y - P_k^{M, N}y)|^2 \\ &\leq mc\{|\mathcal{D}_r(y - P_k^{M, N}y)|^2 + |\mathcal{D}_\theta(y - P_k^{M, N}y)|^2\} \end{aligned} \quad (96)$$

where  $P_k^{M, N}$  was defined in Lemma 3 and (83) was used to establish the last inequality.

We consider part (a). For  $k = 1$  and  $(E, f) \in Q_1 \times \mathcal{F}_1$ , we may use the fact that  $y \in H^2(\Omega)$  (Corollary 1) and estimates (94), (95) and (75) to claim that the bound in (96) becomes

$$\begin{aligned} |\nabla(y - y_1^{M, N})|^2 &\leq 2C_1^2(MN)^{-2} \frac{mc}{m} |\mathcal{D}^2y|^2 \\ &\leq C(MN)^{-2}(|f| + |E|_1 + |y|)^2 \end{aligned}$$

for some constant  $C$ . From the definitions of  $Q_1$ ,  $\mathcal{F}_1$  and the a priori bound (77) on  $y$  (uniform in  $(E, f)$ ) we thus have that

$$|\nabla(y - y_1^{M, N})|^2 \leq \hat{C}(MN)^{-2}$$

for some constant  $\hat{C}$ , where  $\hat{C}$  is determined independent of  $M$ ,  $N$ ,  $E$  and  $f$ .

Therefore,  $|\nabla T^{-1}(y - y_1^{M, N})|^2 = O((MN)^{-2})$  so that (writing  $y$ ,  $y_1^{M, N}$  for  $T^{-1}y$ ,

$T^{-1}y_1^{M,N}$ ),  $y_1^{M,N} \rightarrow y$  in  $H_0^1(\tilde{\Omega})$  as  $M,N \rightarrow \infty$ , uniformly in  $(E,f) \in Q_1 \times F_1$ . Hence part (a) obtains.

To prove part (b), we repeat the above arguments for the case of  $k = 1$  and similarly obtain the convergence of  $y_1^{M,N}$  to  $y$  in  $H_0^1(\tilde{\Omega})$ , for fixed  $(E,f) \in Q_2 \times F_2$ . To consider the case of cubic spline approximations ( $k = 3$ ), we note that  $(E,f) \in Q_3 \times F_3$  implies that  $y \in H^4(\Omega)$  (Theorem 2) and that, following (96) and the arguments for part (a),

$$\begin{aligned} |\nabla(y - y_3^{M,N})|^2 &\leq 2C_1^2(MN)^{-6} \frac{mc}{m} |\mathcal{D}^4 y|^2 \\ &\leq C(MN)^{-6} (|f|_2 + |E|_3 + |y|)^2 \end{aligned}$$

using (76) to obtain the second bound. Using (77) and the definitions of  $Q_3, F_3$ , we are able to claim that

$$|\nabla(y - y_3^{M,N})|^2 \leq \hat{C}(MN)^{-6}$$

so that  $y_3^{M,N} \rightarrow y$  in  $H_0^1(\tilde{\Omega})$  uniformly in  $(E,f) \in Q_3 \times F_3$ . The proof of part (b) is then complete.

Theorem 3: (a) Let  $Q_1 \times F_1$  be compact in the  $L_\infty \times L_2$  topology. For each  $M,N$  there exists a solution  $(\bar{E}^{M,N}, \bar{f}^{M,N})$  to the problem of minimizing  $J_1^{M,N}$  over  $Q_1 \times F_1$ . In addition, there exists  $(\bar{E}, \bar{f}) \in Q_1 \times F_1$  and a subsequence (relabelling)  $\{(\bar{E}^{M_j,N_j}, \bar{f}^{M_j,N_j})\}$  of  $\{(\bar{E}^{M,N}, \bar{f}^{M,N})\}$  such that  $(\bar{E}^{M_j,N_j}, \bar{f}^{M_j,N_j}) \rightarrow (\bar{E}, \bar{f})$  in  $L_\infty \times L_2$ ,  $y^{M_j,N_j}(\bar{E}^{M_j,N_j}, \bar{f}^{M_j,N_j}) \rightarrow y(\bar{E}, \bar{f})$  in  $H_0^1(\tilde{\Omega})$ , and  $(\bar{E}, \bar{f})$  is a solution to the original problem of minimizing  $J$  over  $Q_1 \times F_1$ .

(b) Let  $k = 1$  or  $3$ . Let  $Q_1 \times \mathcal{F}_1$  be compact in the  $L_2 \times L_2$  topology and  $(\bar{E}^{M,N}, \bar{f}^{M,N})$  a solution to the problem of minimizing  $J_k^{M,N}$  over  $Q_1 \times \mathcal{F}_1$ . There exists  $(\bar{E}, \bar{f}) \in Q_1 \times \mathcal{F}_1$  and a subsequence  $\{(\bar{E}^{M_j, N_j}, \bar{f}^{M_j, N_j})\}$  such that  $(\bar{E}^{M_j, N_j}, \bar{f}^{M_j, N_j}) \rightarrow (\bar{E}, \bar{f})$  in  $L_2 \times L_2$ . If in addition  $(\bar{E}, \bar{f}) \in Q_2 \times \mathcal{F}_2$ , then  $y_1^{M_j, N_j}(\bar{E}^{M_j, N_j}, \bar{f}^{M_j, N_j}) \rightarrow y(\bar{E}, \bar{f})$  in  $H_0^1(\Omega)$  and  $(\bar{E}, \bar{f})$  is a solution to the original parameter estimation problem of minimizing  $J$  over  $Q_1 \times \mathcal{F}_1$ . If  $(\bar{E}, \bar{f}) \in Q_3 \times \mathcal{F}_3$ , the same statement may be made in the case of  $k = 3$  (cubic spline approximations).

Proof: It is easy to argue, as in the proof of Lemma 2(a), that

$(E, f) \rightarrow y_1^{M,N}(E, f)$  is continuous in the  $L_\infty \times L_2$  topology, so that  $J_1^{M,N}$  is continuous over the compact set  $Q_1 \times \mathcal{F}_1$ . Thus, for each  $M, N$ , there exists a solution  $(\bar{E}^{M,N}, \bar{f}^{M,N})$  to the approximate parameter estimation problem. From the compactness of  $Q_1 \times \mathcal{F}_1$ , there exists a subsequence  $\{(\bar{E}^{M_j, N_j}, \bar{f}^{M_j, N_j})\}$  and an element  $(\bar{E}, \bar{f}) \in Q_1 \times \mathcal{F}_1$  such that  $(\bar{E}^{M_j, N_j}, \bar{f}^{M_j, N_j}) \rightarrow (\bar{E}, \bar{f})$  in  $L_\infty \times L_2$  and, from Theorem 2,  $y_1^{M_j, N_j}(\bar{E}^{M_j, N_j}, \bar{f}^{M_j, N_j}) \rightarrow y(\bar{E}, \bar{f})$  in  $H_0^1(\Omega)$ . Finally,

$$\begin{aligned} J(\bar{E}, \bar{f}) &= \lim_{M_j, N_j \rightarrow \infty} J_1^{M_j, N_j}(\bar{E}^{M_j, N_j}, \bar{f}^{M_j, N_j}) \\ &\leq \lim_{M_j, N_j \rightarrow \infty} J_1^{M_j, N_j}(E, f) \\ &= J(E, f) \end{aligned}$$

for any  $(E, f) \in Q_1 \times \mathcal{F}_1$ , where we have used Theorem 2(a) and the fact that  $(\bar{E}^{M_j, N_j}, \bar{f}^{M_j, N_j})$  is a minimizer for  $J_1^{M_j, N_j}$  over  $Q_1 \times \mathcal{F}_1$ . Therefore,  $(\bar{E}, \bar{f})$  is a solution to the original parameter estimation problem.

To prove part (b), we duplicate the above arguments for both linear and cubic spline approximations, applying Theorem 2(b) and the  $L_2$  topology on  $Q_2$  ( $Q_3$ ) throughout.

Before our theoretical justification of the spline-based estimation scheme is complete, we must indicate one final result that focuses on the means by which we solve the  $(M, N)$ -th approximate parameter estimation problem. It is implicitly assumed, in the previous calculations that we are able to compute  $(\bar{E}^{M, N}, \bar{f}^{M, N})$ , a solution to the problem of minimizing  $J_k^{M, N}$  over a suitable parameter set  $Q \times F$ . In fact, the sets  $Q \times F$  considered here are infinite-dimensional so that we must perform the minimization over a function space. To implement the approximate estimation scheme, we actually parametrize  $E$  and  $f$  and minimize  $J_k^{M, N}$  over a finite dimensional set  $Q^{I, J} \times F^{I, J}$ . To see how  $(\bar{E}^{M, N, I, J}, \bar{f}^{M, N, I, J})$  (a solution to this problem) approximates  $(\bar{E}, \bar{f})$ , we are forced to consider the limit of such a sequence as  $M, N, I, J \rightarrow \infty$ . That we actually obtain the theoretical convergence of such a sequence (or subsequence) is an easy extension of the ideas in [15a]; these techniques have already been successfully implemented and are described, for the case of the antenna problem, in section IV.

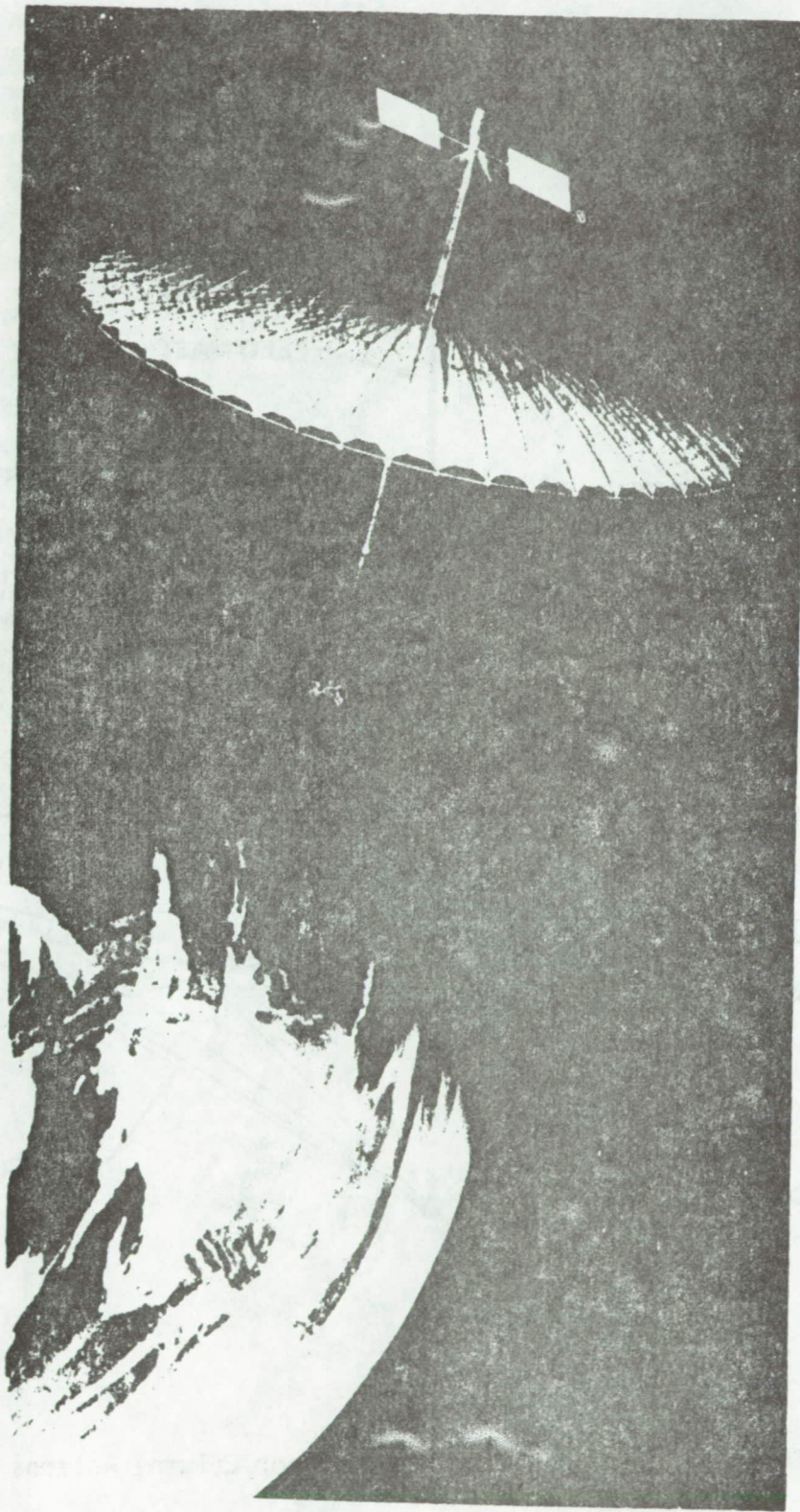


FIGURE 1. Deployed Maypole (Hoop/Column) Antenna

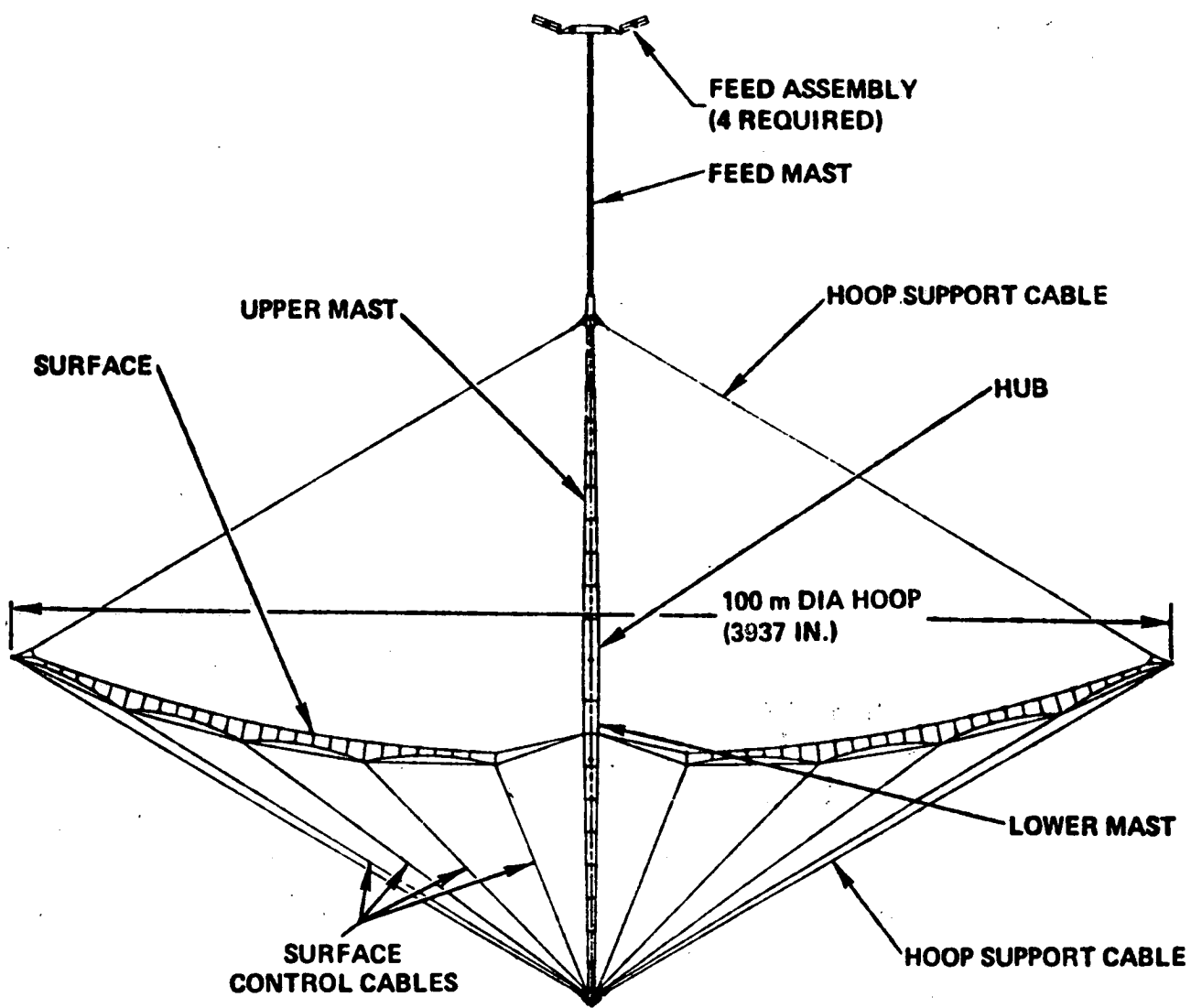


FIGURE 2. Side View of Maypole (Hoop/Column) Antenna

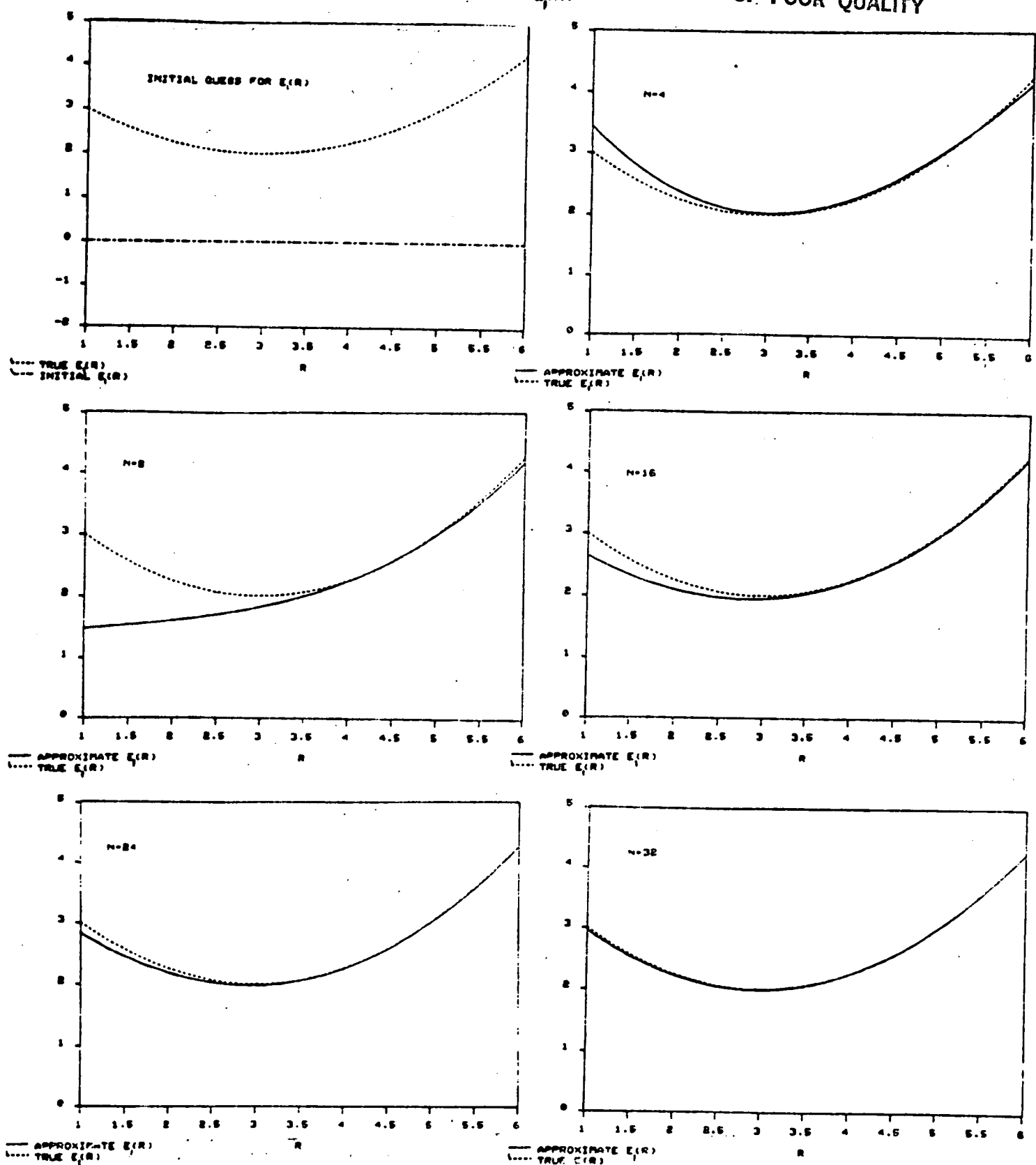


Figure 3: Example 1.1

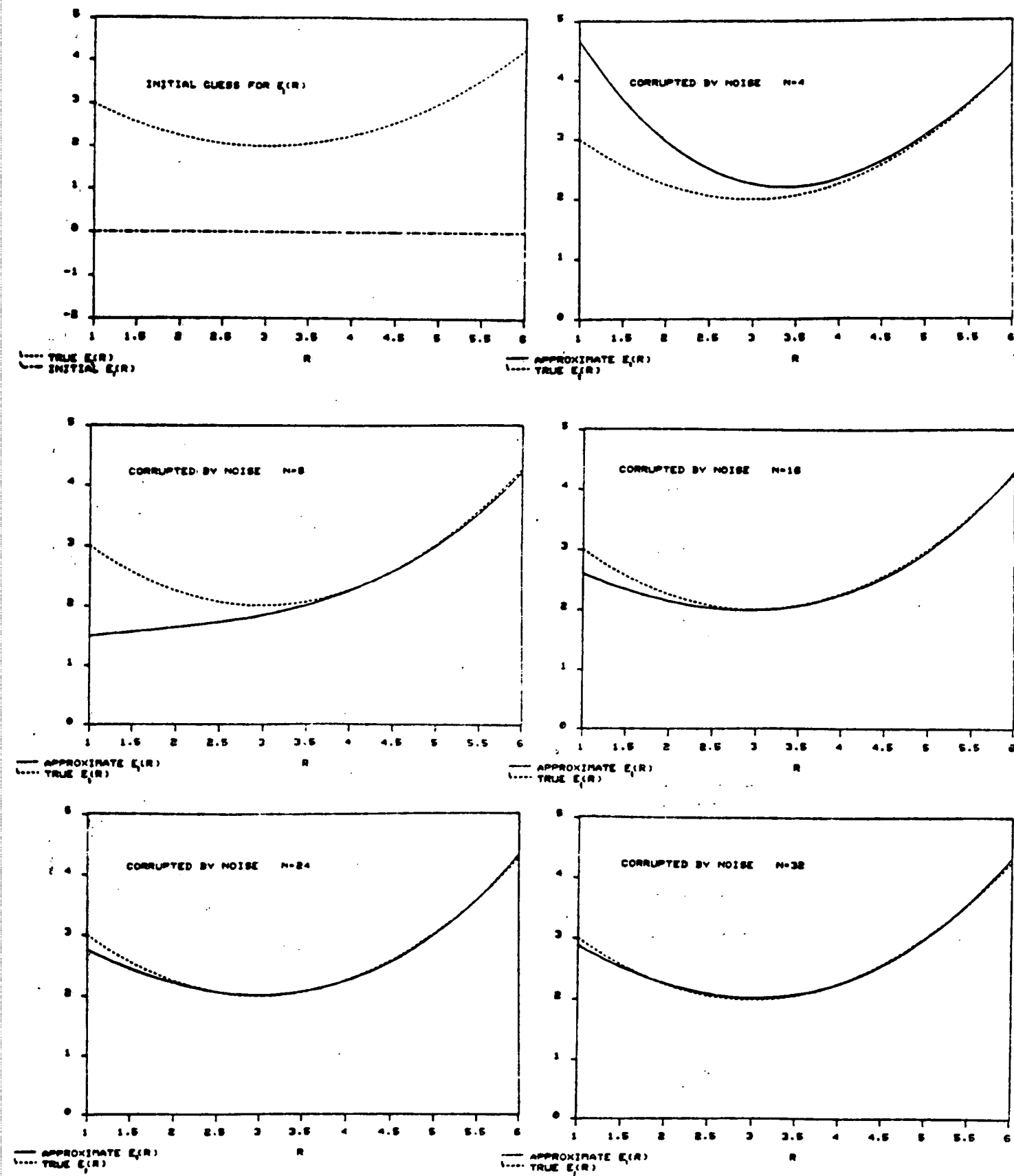


Figure 4: Example 1.2

ORIGINAL PAGE IS  
OF POOR QUALITY

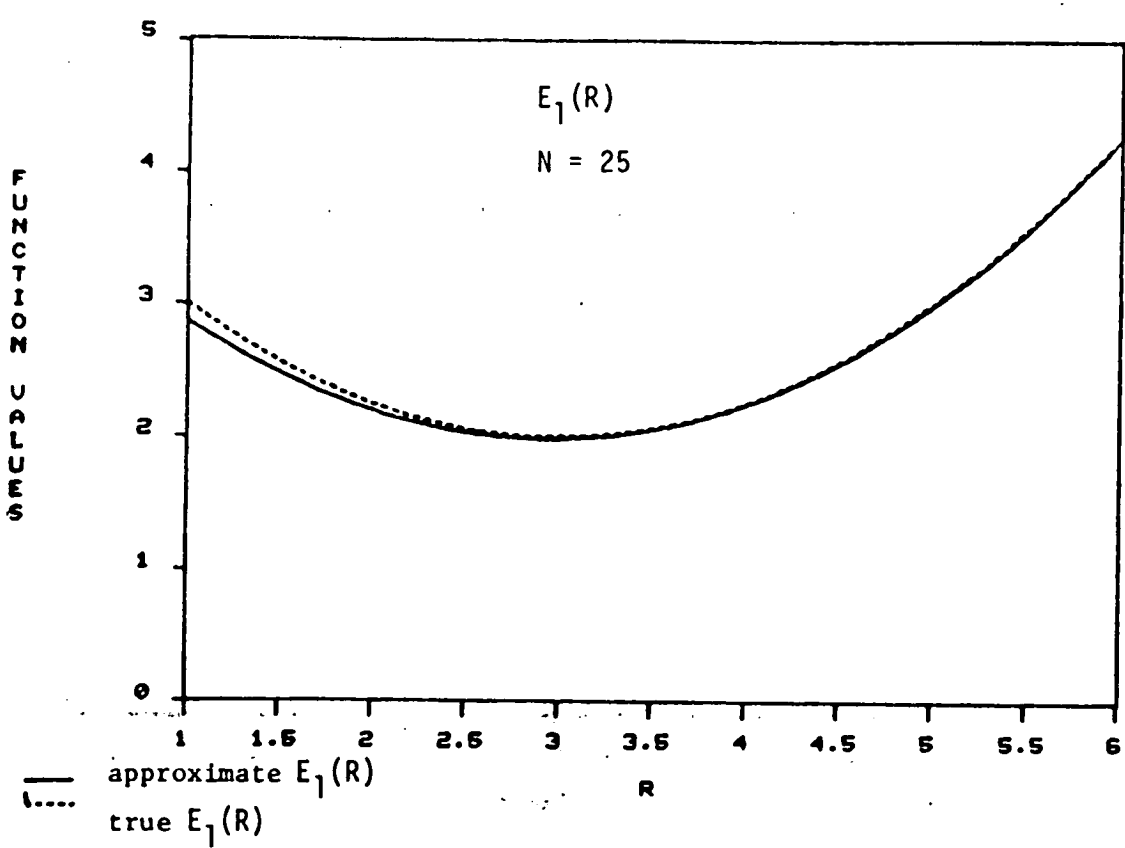
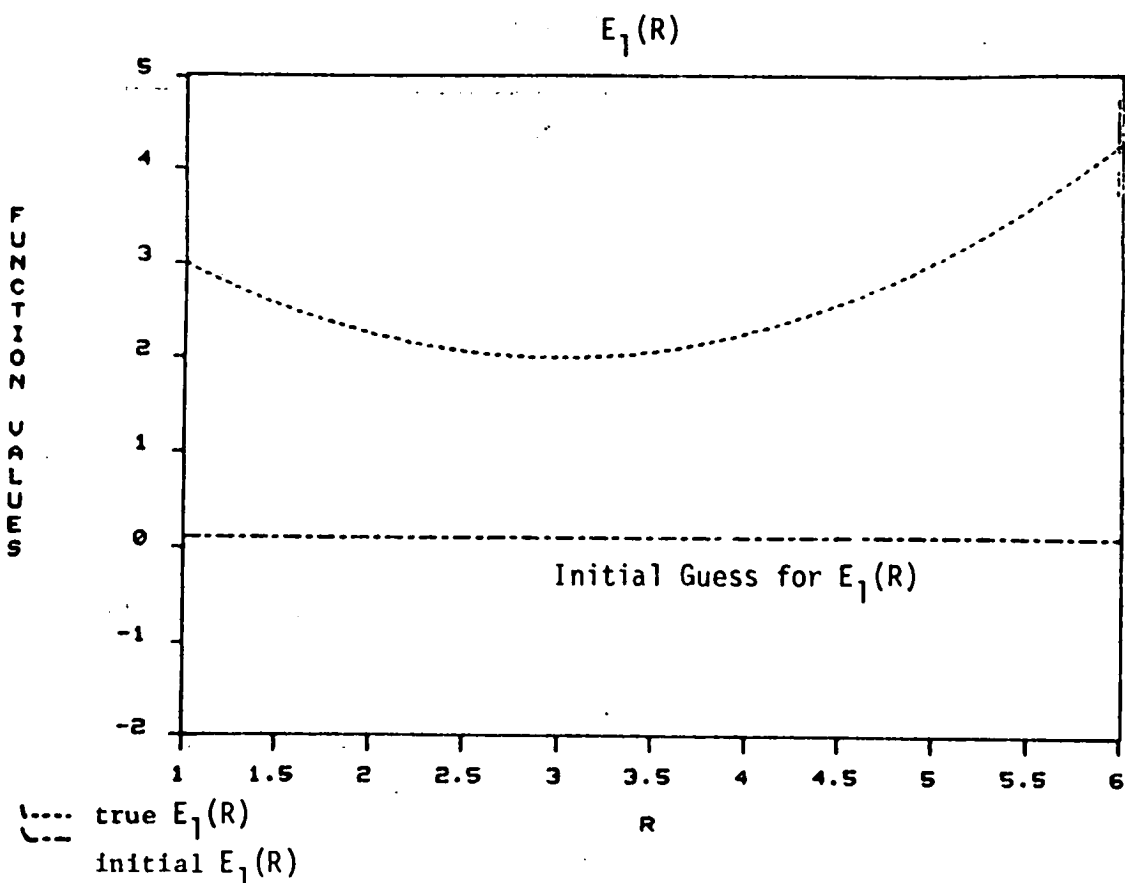


Figure 5(a): Example 1.3

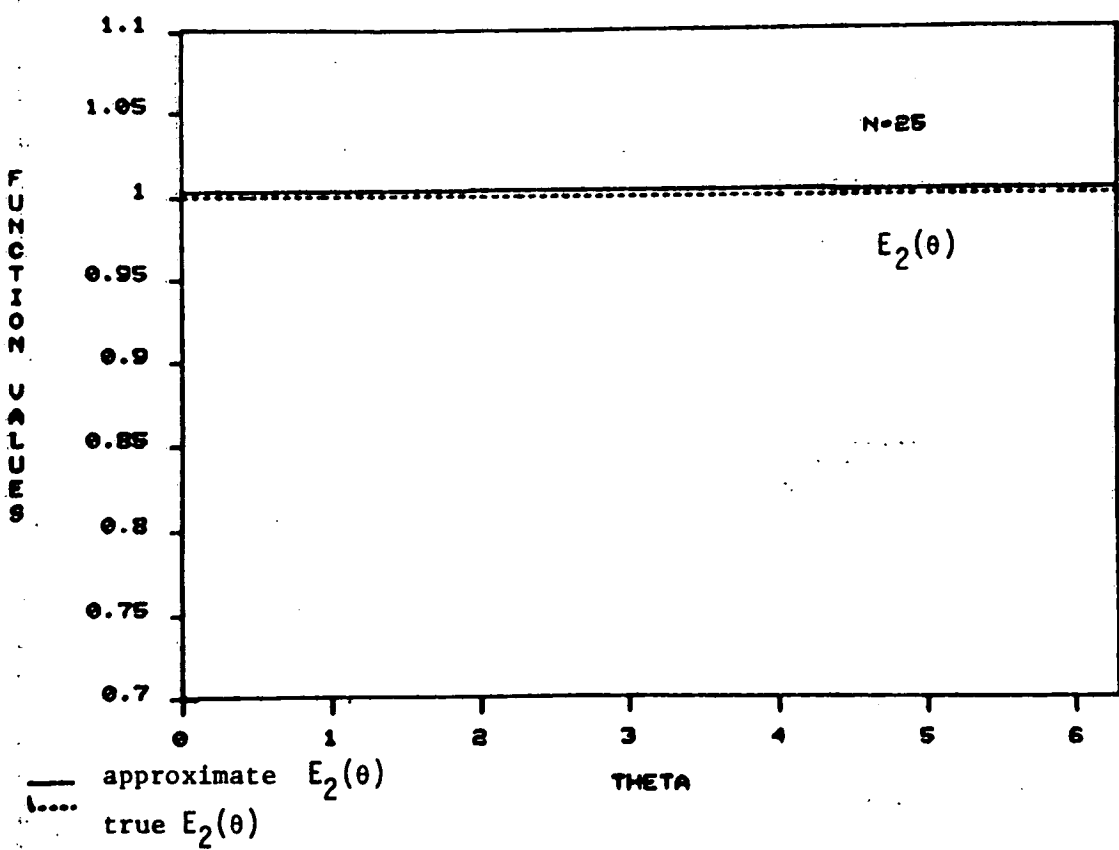
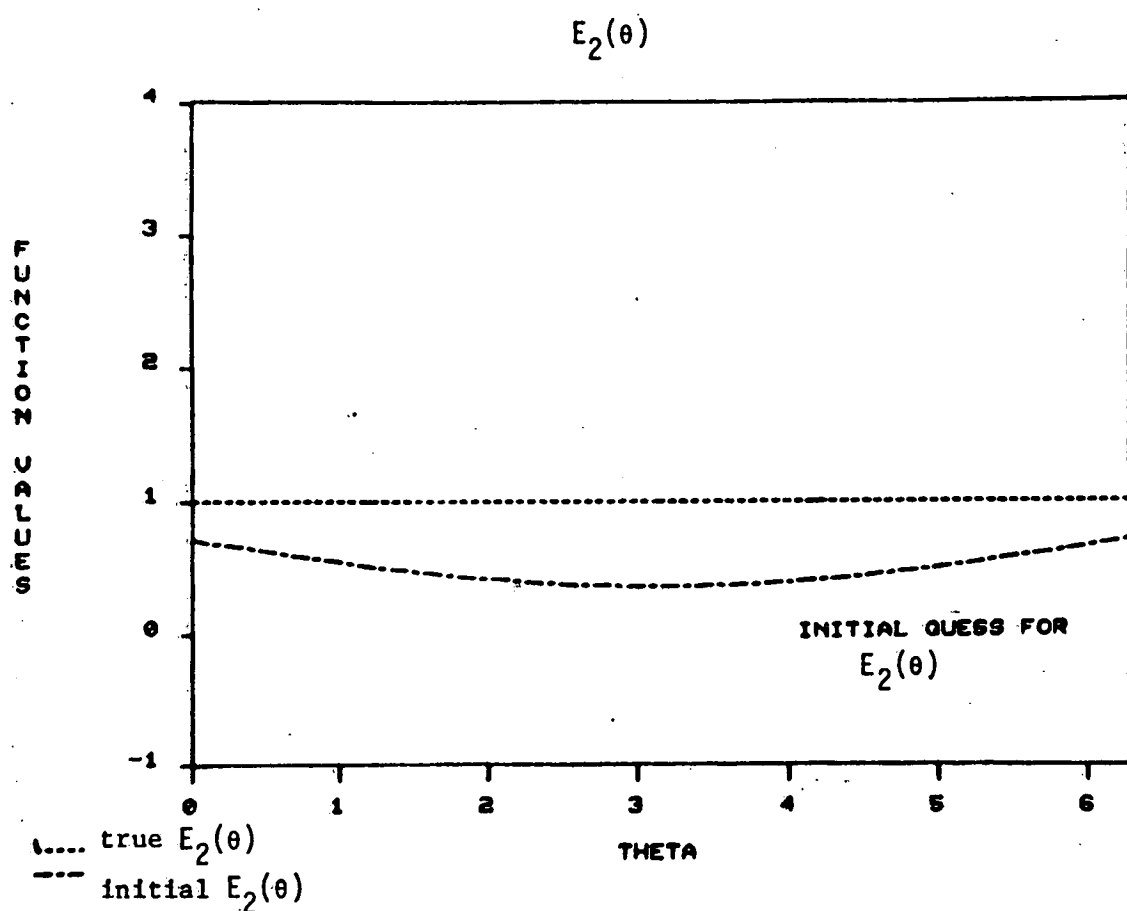


Figure 5(b): Example 1.3

ORIGINAL PAGE IS  
OF POOR QUALITY

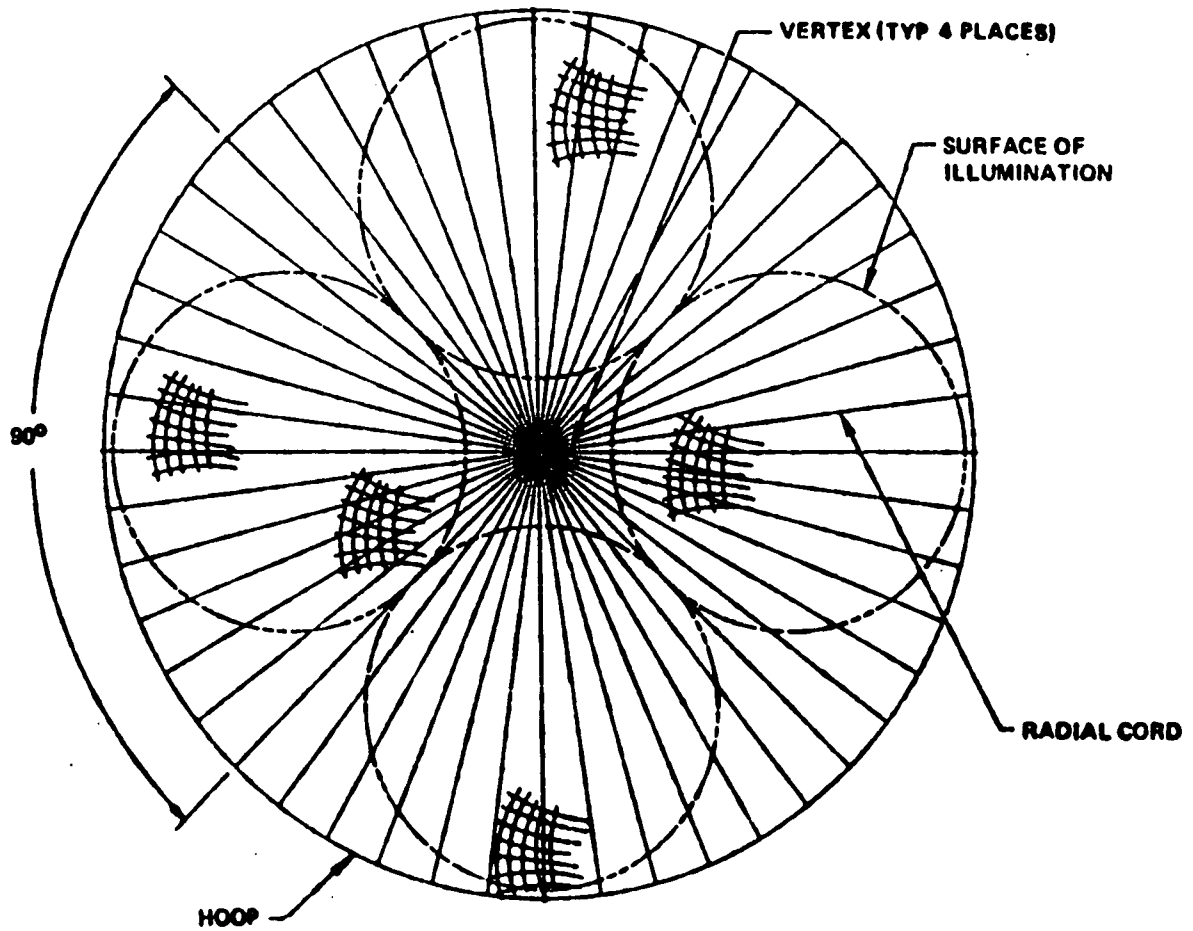


FIGURE 6. Maypole Hoop/Column Antenna Reflector Surface

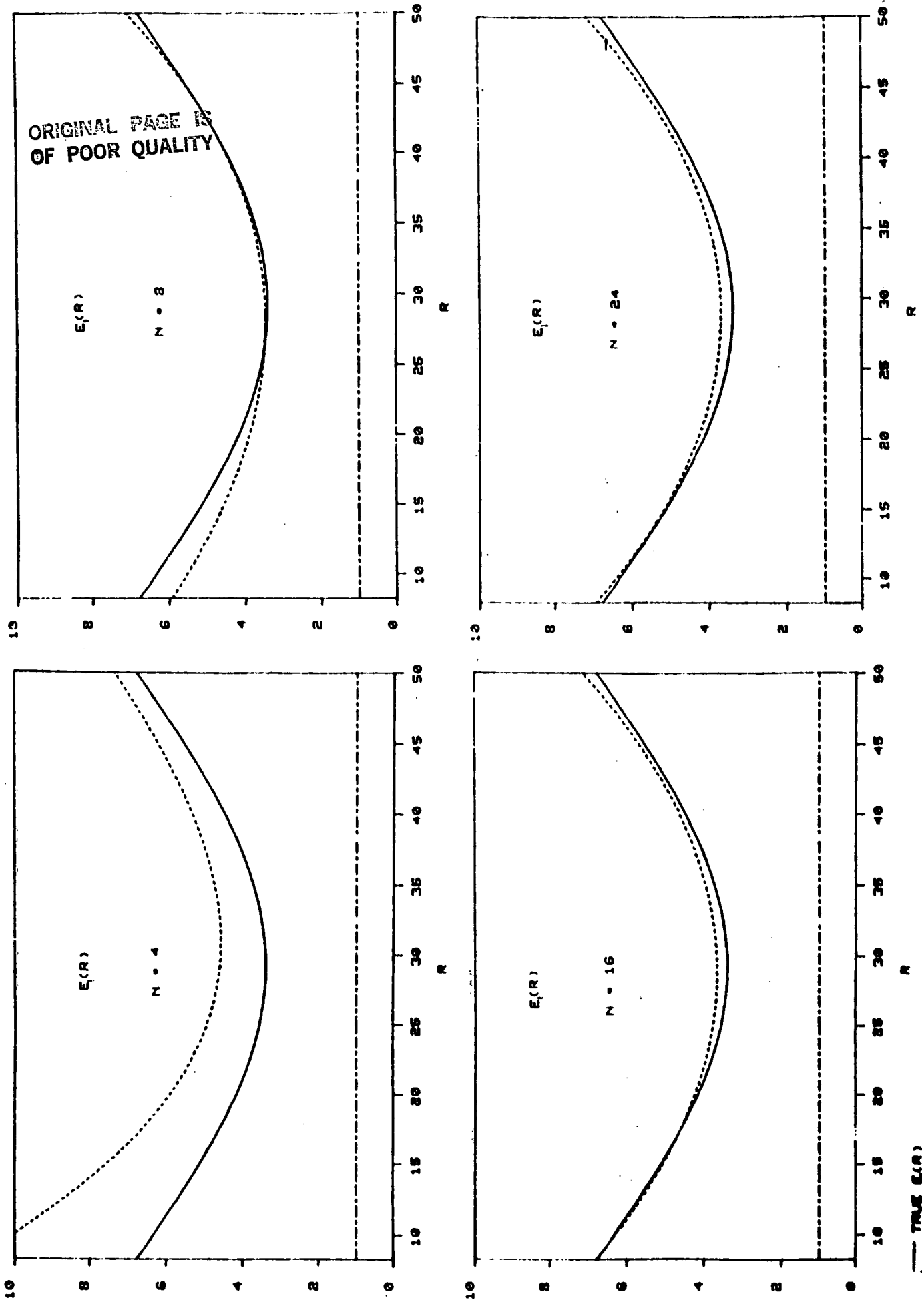


Figure 7: Example 3.2

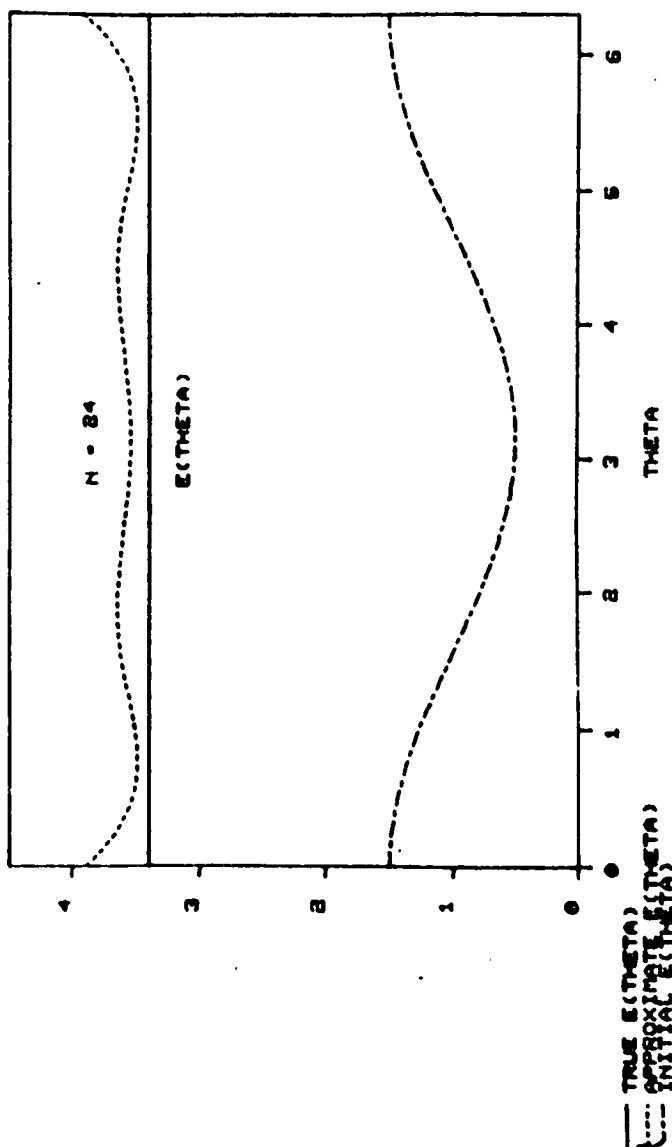
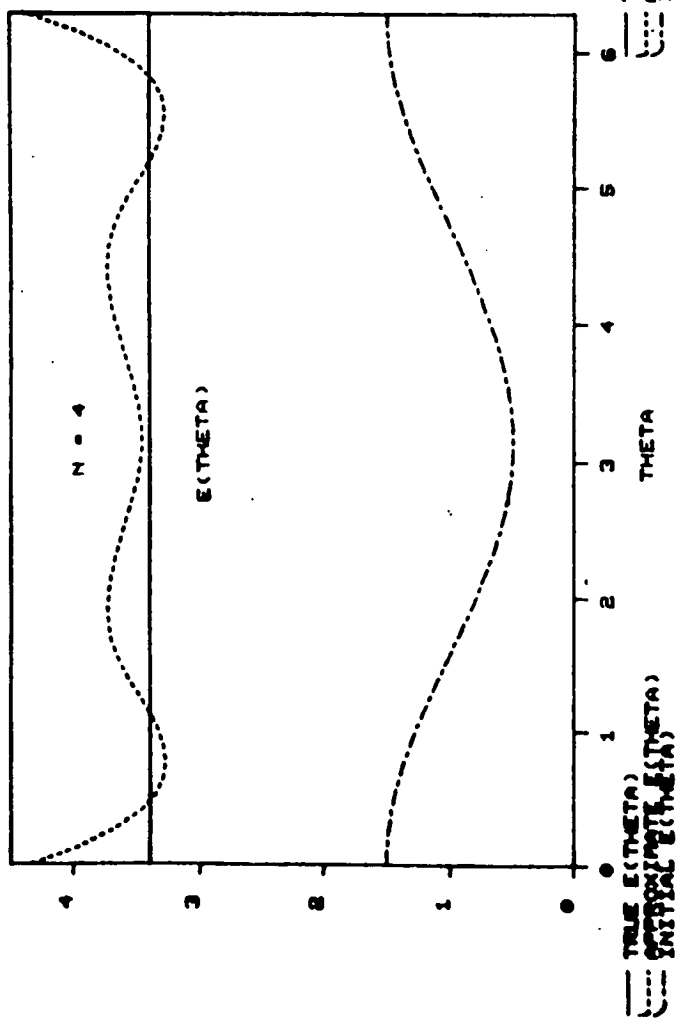
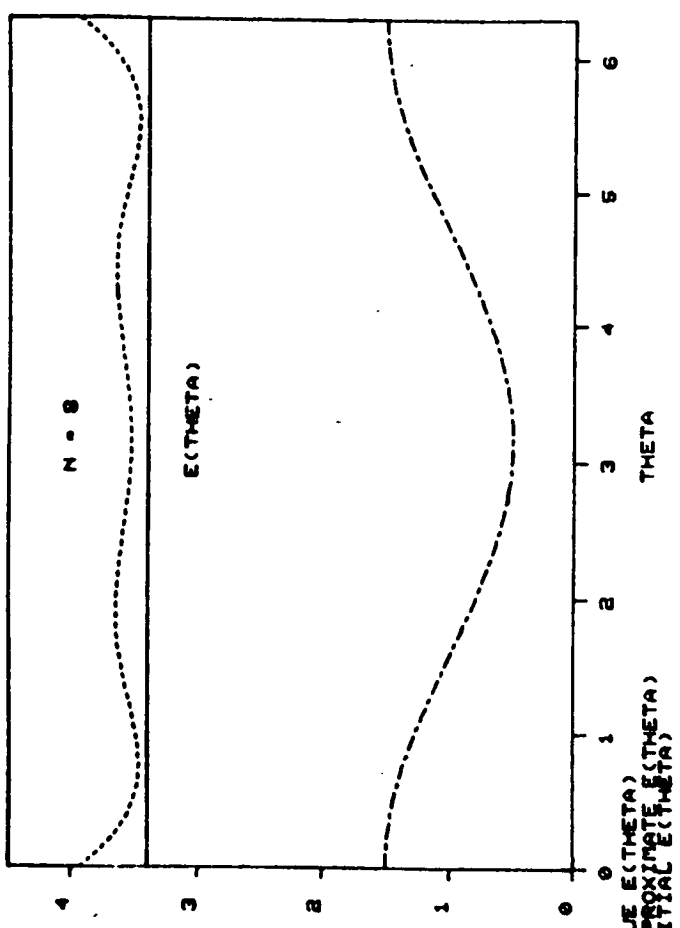
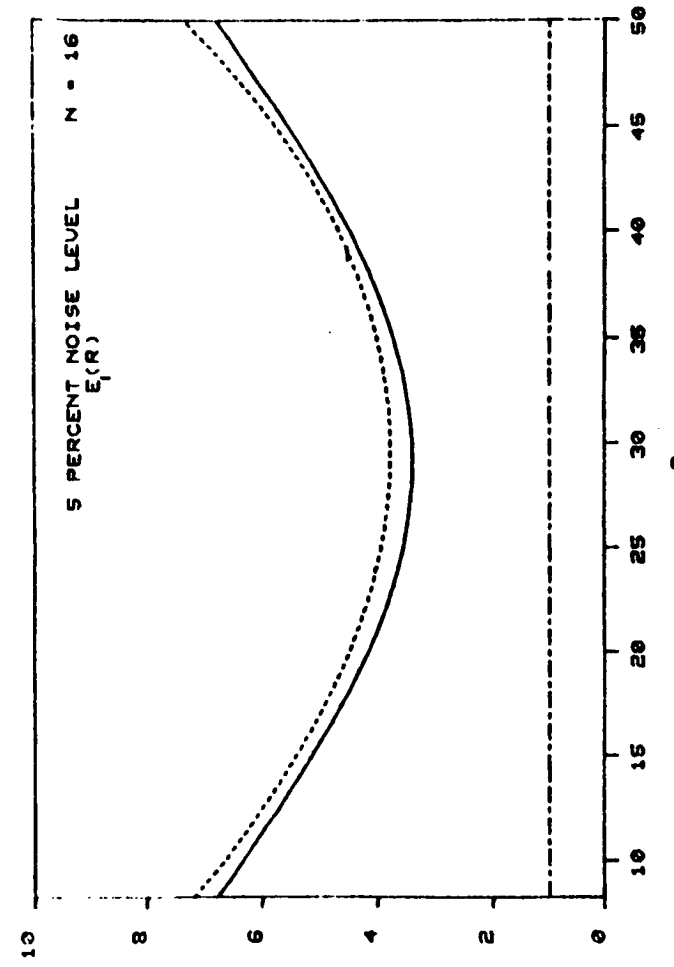
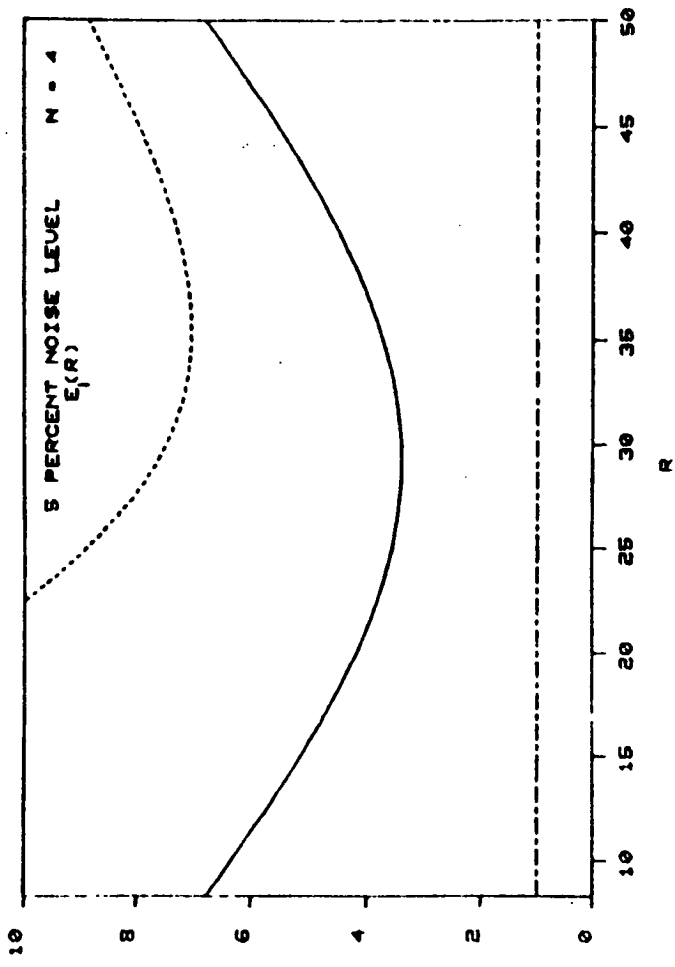
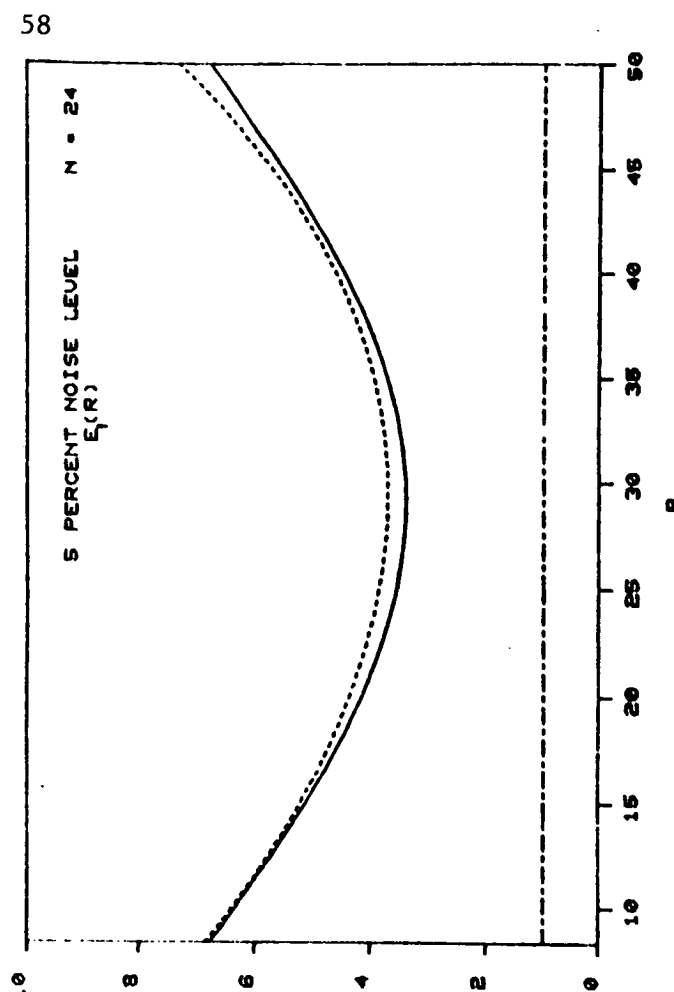
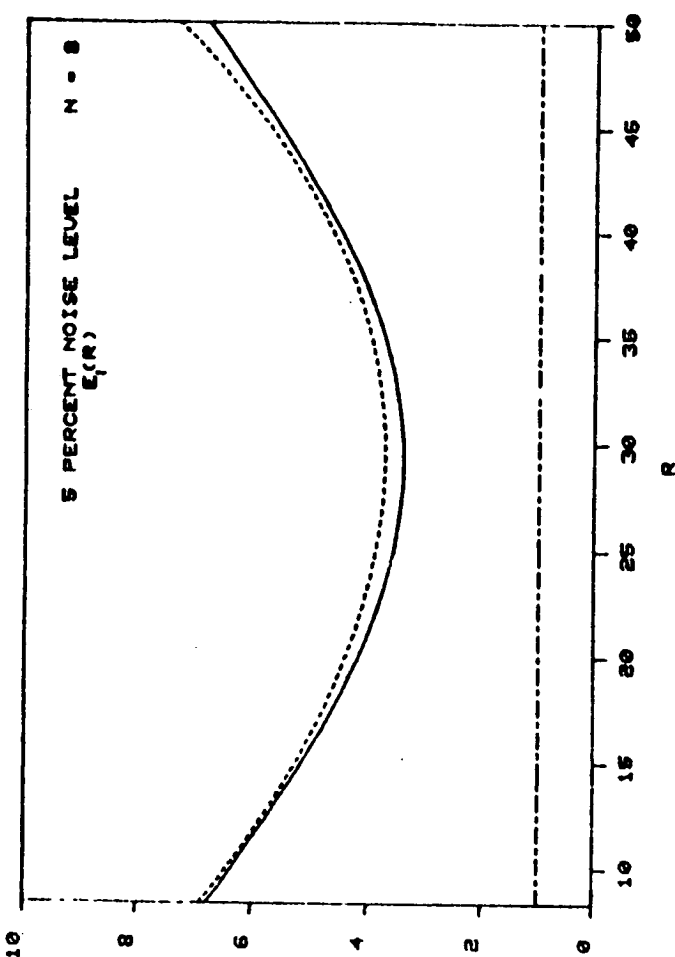


Figure 8: Example 3.3  $E_2(\theta)$



— TRUE  $E_1(R)$   
 - - APPROXIMATE  $E_1(R)$

Figure 9: Example 3.5

## References

- [1] M. J. Balas, Trends in large space structure control theory: fondest hopes, wildest dreams. IEEE Trans. Auto. Control, Vol. AC-27, (June, 1982), 522-535.
- [2] P. C. Hughes, Passive dissipation of energy of large space structures, J. Guidance Contr., Vol. 3, (1980), 380-382.
- [3] R. Gran and M. Rossi, A survey of the large structures control problem, Presented at IEEE Decision and Control Conference, Ft. Lauderdale, FL, 1979.
- [4] J. L. Lions, Optimal Control of Systems Governed by Partial Differential Equations. Springer-Verlag, New York, 1971.
- [5] D. Russell, Controllability and stabilizability theory for linear PDE's: Recent progress and open questions. SIAM Rev., Vol. 20, (1978), 639-739.
- [6] A. V. Balakrishnan, Applied Functional Analysis. Springer-Verlag, 1976.
- [7] R. F. Curtain and A. J. Pritchard, Infinite Dimensional Linear System Theory. Springer-Verlag, 1978.
- [7a] W. H. Ray and D. G. Lainiotis, Eds., Distributed Parameter Systems: Identification, Estimation, and Control. Marcel Dekker, New York, 1978.
- [7b] J. S. Gibson, The Riccati integral equations for optimal control problems on Hilbert spaces, SIAM J. Control Optimiz. 17 (1979), 537-565.
- [7c] J. S. Gibson, An analysis of optimal modal regulation: convergence and stability, SIAM J. Control Optimiz. 19 (1981), 686-707.
- [8] Special Issue on Linear Multivariable Control Systems. IEEE Trans. Auto. Control, AC-26, (February, 1981).
- [9] R. A. Russell, T. G. Cambell and R. E. Freeland, A technology development program for large space antennas. Paper No. IAF-80A33, presented at Thirty-First International Astronautical Congress of the International Astronautical Federation, Tokoyo, Japan, Sept. 21-28, 1980.
- [10] M. P. Polis and R. E. Goodson, Parameter identification in distributed systems: A synthesizing overview. Proceedings of the IEEE, 64, (January, 1976), 45-60.
- [11] H. T. Banks, Algorithms for estimation in distributed models with applications to large space structures. Proc. Workshop on Applications of Distributed System Theory to the Control of Large Space Structures, JPL-Calif. Inst. Tech, Pasadena, CA, July 14-16, 1982.

- [12] H. T. Banks and J. M. Crowley, Parameter estimation in Timoshenko beam models. Lefschetz Center for Dynamical Systems Report No. 82-14, Brown University, Providence, RI, June, 1982; to appear in J. Astronautical Sci.
- [13] H. T. Banks, J. M. Crowley and K. Kunisch, Cubic spline approximation techniques for parameter estimation in distributed systems. Lefschetz Center for Dynamical Systems Report 81-25, Brown University, Providence, RI, 1981; to appear in IEEE Trans. Auto. Control.
- [14] H. T. Banks and P. L. Daniel, Parameter estimation of nonlinear non-autonomous distributed systems. Proc. 20th IEEE Conf. on Decision and Control, San Diego, CA, Dec. 16-18, 1981, 228-232.
- [15] H. T. Banks and K. Kunisch, An approximation theory for nonlinear partial differential equations with applications to identification and control. Lefschetz Center for Dynamical Systems Report 81-7, Brown University, Providence, RI, 1981; SIAM J. Control and Optimization, 20 (1982) 815-849.
- [15a] H. T. Banks and P. L. Daniel, Estimation of variable coefficients in parabolic distributed systems, LCDS Rep. #82-22, Sept., 1982, Brown University.
- [16] M. R. Sullivan, LSST (Hoop/Column) Maypole Antenna Development Program, Parts I and II. NASA CR 3558, June, 1982.
- [16a] H. T. Banks and G. Majda, Modeling of flexible surfaces: a preliminary study, ICASE Rep., Hampton, VA, May, 1983.
- [17] H. Sagan, Boundary and Eigenvalue Problems in Mathematical Physics. John Wiley & Sons, Inc., 1966.
- [17a] G. Rodriguez, Optimal control of large structures modeled by partial differential equations, Proc. AIAA Guidance and Control Conf., August 6-8, 1979, Boulder, CO.
- [17b] C. J. Weeks, Shape determination and control for large space structures, JPL Publication 81-71, October, 1981, Jet Propulsion Lab, Pasadena, CA.
- [18] H. T. Banks, Distributed system optimal control and parameter estimation: computational techniques using spline approximations. Lefschetz Center for Dynamical Systems Rep. 82-6, Brown University, Providence, RI, 1982; in Proc. 3rd IFAC Symposium on Control of Distributed Parameter Systems, Toulouse, France, June 29 - July 2, 1982, S.P.21-S.P.27.
- [18a] H. T. Banks, A survey of some problems and recent results for parameter estimation and optimal control in delay and distributed parameter systems, in Volterra and Functional Differential Equations, (K. B. Hannsgen, et al., eds.), Marcel Dekker, New York, 1982, 3-24.

- [19] H. T. Banks, P. L. Daniel and E. S. Armstrong, Parameter estimation for static models of the Maypole Hoop/Column antenna surface, Proceedings of IEEE Int'l Large Scale Systems Symposium, Va. Beach, VA, October 11-13, 1982, 253-255.
- [20] G. Strang and G. J. Fix, An Analysis of the Finite Element Method, Prentice-Hall, Inc., 1973.
- [20a] M. H. Schultz, Spline Analysis, Prentice-Hall, Englewood Cliffs, N. J., 1973.
- [21] P. Lancaster, Theory of Matrices. Academic Press, Inc., 1969.
- [22] R. H. Bartels and G. W. Stewart, Algorithm 432 - A solution of the matrix equation  $AX + XB = C$ . Commun. ACM, Vol. 15, (Sept. 1972), 820-826.
- [23] J. J. More, The Levenberg-Marquardt Algorithm, Implementation and Theory in Numerical Analysis, (G. A. Watson, ed.), Lecture Notes in Mathematics 630, Springer-Verlag, 1977.
- [24] A. Friedman, Partial Differential Equations of Parabolic Type, Prentice-Hall, Englewood Cliffs, N.J., 1964.
- [25] A Friedman, Partial Differential Equations, Robert E. Krieger Publishing Co., Huntington, N.Y., 1976.
- [26] R. A. Adams, Sobolev Spaces, Academic Press, N. Y., 1975.
- [27] W. Fleming, Functions of Several Variables, Springer-Verlag, N.Y., 1977.